Transport processes during the growth of oxide films at elevated temperature

A. Atkinson

Materials Development Division, Building 552, AERE Harwell, Didcot OX11 0RA, England

The current understanding of the growth of thermal oxide films in terms of the transport properties of the oxides is reviewed. Emphasis is placed on examining quantitative relationships between the film growth rate and other measurable parameters of the oxides. The theories of film growth which are expected to apply in the extreme limits of thick films (Wagner) and thin films (Cabrera and Mott) are outlined. Particular attention is given to examining the expected limits of validity of these theories and to the various ways in which their predictions can be tested experimentally. The growth of a selection of important oxides is then discussed in the light of these two theories. The examples (CoO, NiO, Fe_3O_4, Cr_2O_3, Al_2O_3, and SiO_2) have been selected such that together they serve to test the theories, have technological relevance, and exhibit a wide variation in behavior. The dominant role of diffusion along oxide grain boundaries in controlling the growth of the crystalline oxides is highlighted.

CONTENTS

I. Introduction 437
II. Theory of Oxide Film Growth 438
A. Theory of thick film growth 438
1. Wagner theory for thick films 438
2. Thick film growth in terms of point defects 440
3. Expected range of validity of Wagner's theory 441
B. Theory of thin film growth 442
1. Oxide defects injected at the metal/oxide interface 443
2. Oxide defects injected at the oxide/gas interface 444
C. Comparing theory with experiment 444
1. Thick films (Wagner) 445
2. Thin films (Cabrera and Mott) 445
D. Atom tracers in growing films 447
E. Less restrictive theories of film growth 448
III. Growth of Some Selected Oxides 449
A. Growth of CoO 449
B. Growth of NiO 450
1. Growth of thick NiO films at $T > 500\,^{\circ}C$ 450
2. Growth of thin NiO films at $T < 500\,^{\circ}C$ 452
C. Growth of iron oxides 454
D. Growth of Cr_2O_3 455
1. Growth of thick Cr_2O_3 films 455
2. Growth of thin Cr_2O_3 films 456
E. Growth of Al_2O_3 films 457
IV. Oxidation of Silicon 459
A. Growth of thick SiO_2 films in O_2 459
B. Growth of thin SiO_2 films in O_2 461
C. Growth of thick SiO_2 films in H_2O 462
V. Duplex and Lateral Film Growth 464
A. Growth of duplex films 464
B. Lateral film growth 466
VI. Summary and Conclusions 467
Acknowledgments 468
References 468

I. INTRODUCTION

The purpose of this paper is to review the current state of understanding of the growth of oxide films, by thermal oxidation, in terms of transport processes taking place within the growing films. Such films may be formed as a result of a "corrosion" process causing unwanted loss of metal from an engineering component. They may alternatively be deliberately formed under certain conditions in order to protect a metal from rapid corrosion in more aggressive conditions. This is often the case with films of Cr_2O_3 and Al_2O_3. Or the films may be grown for their useful properties in some very different context, as is the case with SiO_2 films grown on Si in integrated circuit technology.

In order to specify more closely the applicability of the phenomena considered here, it is useful to examine in greater detail some of the terms used in the opening sentence. The term "film" is taken to mean a layer of oxide ranging from a single monolayer to several mm in thickness. Films thicker than $\sim 10\ \mu m$ are often referred to as "scales," but the single term "film" will be used here to cover all cases. The "growth" of such a film must be preceded by the adsorption of molecules from the gas, their dissociation and ionization, their rearrangement to form oxide nuclei, and the lateral growth of the nuclei until they impinge on each other to form a complete layer of oxide. These processes will not be discussed here; only the subsequent thickening of the film is included. By "thermal oxidation" I am restricting the discussion to the basic system, metal substrate/oxide film/oxygen-bearing gas, from room temperature upwards. Other oxidation processes, such as anodic oxidation in an aqueous environment, are not specifically treated. Nevertheless, the basic principles still apply, even though different external conditions will modify the consequences. Similarly, although the discussion will be limited to oxides, the same treatments can be applied to the formation of any binary compound (e.g., a chloride, a sulfide, or a nitride) by a solid-gas reaction, or even a solid-liquid one, or an all solid-state reaction.

The term "understanding" also requires some clarification. Understanding may be sought at both the phenomenological and the atomistic levels; we shall be concerned with both. At the phenomenological level I attempt to relate the rate of film growth to other measurable transport properties of the oxides, such as diffusion coefficients and electronic conductivities. At the atomistic level I try to identify the way in which the ions and electrons move in the rate-controlling processes. These are usually deduced from studies of the transport proper-

ties themselves and concentrate on deciding what defects in the oxide are responsible for transport of ions (e.g., vacancies or interstitials).

The paper is structured in the following way. The theory of oxide film growth is first described. The theories of Cabrera and Mott for the growth of "thin" films and of Wagner, for "thick" films, are summarized, because they are appropriate limiting cases. The current understanding of the growth of some selected oxides (CoO, NiO, Fe oxides, Cr_2O_3, and Al_2O_3) will then be examined in the light of these theories. The oxides have been chosen either because they are important as model oxides for testing the theory, or because they are important in giving protection against high-temperature corrosion. (Because of its usefulness as a model oxide, I have also chosen to use NiO as a standard example for illustration in other parts of the paper.) A complete section is then devoted to the growth of SiO_2 films on Si because of its technological importance, because of the large volume of work on this system, and because it is significantly different from the other oxides. Finally, attention is drawn to some less straightforward growth processes, such as lateral growth and duplex layer growth. The growth of oxides on alloys will not be considered in detail in this paper.

An extensive review of the oxidation of pure metals has been given by Lawless (1974), and there are several articles and books (e.g., Kofstad, 1966) in which the subject is treated in detail. In this review only the minimum of this earlier work necessary to provide an adequate background will be reiterated. Instead, more attention will be given to the relationships between the theories, their limits of application, and more recent experimental data.

In Secs. II, III, and IV I have chosen to discuss the growth of "thick" films before the growth of "thin" films, even though the film must obviously grow through the "thin" regime before it becomes "thick." The reason for this is that the growth of thick films is simpler, better understood, and more readily related to other measurable parameters than the growth of thin films, as I hope will become clear.

II. THEORY OF OXIDE FILM GROWTH

A. Theory of thick film growth

1. Wagner theory for thick films

We shall return later to a more rigorous consideration of the definition of a thick film, but, as a rough guide, films thicker than 1 μm are considered to be thick.

Wagner's (1933) theory of thick film growth provides a means by which the rate of film growth can be related to other measurable transport properties of the film, such as diffusion coefficients. In the period preceding this theory it had been observed that the growth of films (Tammann, 1920) obeyed parabolic kinetics, i.e.,

$$X^2 = k_p t \ , \tag{2.1}$$

where X is the film thickness and k_p is the parabolic rate constant. The parabolic kinetics can be seen to be consistent with the rate of growth being controlled by transport down a gradient of driving force, which becomes proportionally smaller as the film thickness increases, i.e. [by differentiating Eq. (2.1)],

$$\frac{dX}{dt} = \frac{k_p}{2X} \ . \tag{2.2}$$

Thus Wagner's theory is based upon diffusion across the film being the slowest, and therefore the rate-limiting, step in the overall sequence of reactions. Figure 1 shows the different species that may be transported across the film. In general, oxides can be regarded as compounds having predominantly ionic bonding, and therefore, it is appropriate to consider the separate transport of ions and electrons. Whether metal ion transport dominates over that by oxygen ions, or whether electronic currents are carried by electrons or holes, depends on the point defect and electronic structure of the oxide. Nevertheless, there must be both electronic and ionic transport in order to ionize metal and oxygen atoms at the interfaces and provide material transport across the film. Since the diffusing species are electrically charged, their fluxes will be determined both by gradients in chemical potential and by electric fields, which may be developed by a separation of charge. In general for any diffusing species i the particle (or defect) current density is given by

$$J_i = \frac{D_i C_i}{kT}\left[-\frac{d\mu_i}{dx} + q_i E\right] , \tag{2.3}$$

where C_i is their concentration (number of particles per unit volume), μ_i their chemical potential ($=kT\ln C_i$ + const, for ideal noninteracting particles), D_i their diffusion coefficient, and q_i their charge (or effective charge in the case of a defect).

The validity of Eq. (2.3) depends on the validity of the Nernst-Einstein relationship, which has been used to express electrical transport in terms of a diffusion coefficient. This, in turn, assumes that the electrical field is

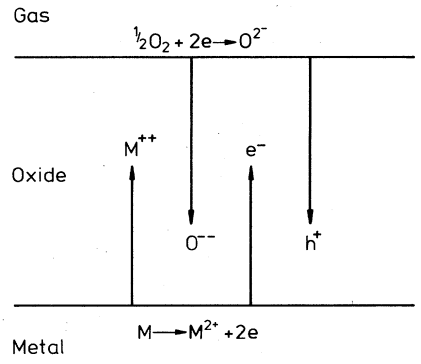

FIG. 1. Transport of ions and electrons in gradients of oxygen activity and electric potential across a growing oxide film.

small, such that $qEa \ll kT$, where a is the ionic jump distance. The electric field developed during thick oxide film growth can be regarded as arising from ambipolar diffusion in the oxide. For example, suppose that metal ions are more mobile in the oxide than are oxygen ions, so that new oxide is formed at the oxide/oxygen interface. Electrons must also diffuse outward with the metal ions (or holes diffuse inward) to ionize the O atoms at the interface that are to be incorporated into the new oxide lattice. If, as is usually the case, the electrons are more mobile than the metal ions, an electric field will develop to speed up the ions and slow down the electrons until the electric currents carried by the two types of charged particle are equal (and opposite). Thus the oxide/gas interface develops a negative electrical potential with respect to the oxide/metal interface. The same is true if the film grows mainly by diffusion of oxygen ions. Thus the sign of the electric field developed in a growing oxide film does not depend on whether oxygen ions or metal ions are the more mobile, but whether the electronic or ionic species are the more mobile.

In the preceding paragraph it was assumed that there should be no net electrical current flowing across the film, and this is also assumed in Wagner's theory. In fact Wagner assumed that the oxidizing system is in a pseudo-steady-state, so that not only is there no electrical current flowing across the whole film, but also there is no electrical current flowing across any elemental thickness of the film. Wagner further assumed that local chemical equilibrium exists throughout the film and that there is no divergence in the ionic and electronic currents. Using these assumptions, he was able to eliminate from the coupled transport equations of the type (2.3) the electric field and all the chemical potentials except one, which is conveniently taken to be the chemical potential of oxygen. The parabolic rate constant was thus expressed in terms of measurable electrical parameters in the following form:

$$k_p = \frac{kT}{4e^2 \alpha N_0} \int_{a(O_2)_I}^{a(O_2)_{II}} t_e t_{ion} \sigma \, d[\ln a(O_2)] , \tag{2.4}$$

where e is the modulus of the electronic charge and N_0 is the number of MO_α molecules per unit volume of oxide. The total electrical conductivity of the oxide is σ, and t_e and t_{ion} are the fractions of total electrical conductivity that are provided by electronic and ionic transport, respectively (transport numbers). The limits of integration in Eq. (2.4) are the activities of molecular oxygen at the metal/oxide interface $[a(O_2)_I]$ and the oxide/gas interface $[a(O_2)_{II}]$. The activity of a perfect gas is equal to its partial pressure in atmospheres.

In most oxides of interest the ionic conductivity is very much less than the electronic conductivity ($t_{ion} \ll t_e \simeq 1$), and it is more convenient to cast Eq. (2.4) in a form that includes the most readily accessible parameters experimentally, i.e., the tracer self-diffusion coefficient (D^*):

$$k_p = \int_{a(O_2)_I}^{a(O_2)_{II}} \left[\alpha \frac{D^*(M)}{f_M} + \frac{D^*(O)}{f_O} \right] d[\ln a(O_2)] . \tag{2.5}$$

In this expression f_M and f_O are the correlation factors for the metal ion and oxygen ion self-diffusion mechanisms and are of the order unity. The importance of Eq. (2.5) is that it expresses a quantitative relationship between the parabolic rate constant for thermal oxidation and the self-diffusion coefficients of the ions in the oxide film. Furthermore, the relationship is a phenomenological one, rather than an atomistic one, since evaluation of k_p from Eq. (2.5) is only weakly dependent on the atomistic diffusion mechanisms through the correlation factors. Evaluation of k_p from Eq. (2.5) merely requires that data exist for the self-diffusion coefficients as a function of $a(O_2)$. However, such data do contain information about the defect structure of the oxide, and, indeed, this has proved to be one of the most fruitful ways of probing the defect structure.

Since the electric field that develops during oxidation is an important feature of the process, considering it in greater detail is worthwhile. The electric field is defined as the negative gradient of the potential energy of a unit test charge, and therefore, there will be a difference in electrostatic potential across the film. However, the "test charges" that are employed in practical voltmeters are electrons, which are not inert. Furthermore, the voltmeter must use electrodes to contact the specimen, and these will have their own electronic and ionic conducting properties. It can be shown (e.g., Kröger, 1974, Chap. 24.2) that the electrostatic potential difference between the two interfaces is given by

$$\varphi_{II} - \varphi_I = \frac{kT}{4e} \int_I^{II} t_i d \ln[a(O_2)] + \frac{1}{e}[\mu(e)_{II} - \mu(e)_I] , \tag{2.6}$$

where $\mu(e)$ is the chemical potential of an electron and I and II denote the metal/oxide and oxide/gas interfaces.

If the voltage is probed with electronically conducting electrodes that are chemically inert (e.g., Pt), then the voltage $\mathscr{V}_e$ is the difference in the electrochemical potential of electrons between electrodes II and I (divided by $-e$). Since the electrochemical potential of an electron is $\mu(e) - e\varphi$, it follows that

$$\mathscr{V}_e = \frac{kT}{4e} \int_I^{II} t_{ion} d[\ln a(O_2)] . \tag{2.7}$$

If t_{ion} is independent of oxygen activity, then (2.7) can be integrated to give

$$\mathscr{V}_e = -\frac{\Delta G_{MO_\alpha}}{2e\alpha} t_{ion} , \tag{2.8}$$

where ΔG_{MO_α} is the free energy of formation of a molecule of MO_α from oxygen of activity $a(O_2)_{II}$. Thus we see that although the sign of $\varphi_{II} - \varphi_I$ depends on whether $t_{ion} > t_e$ (as mentioned previously), the sign of the voltage measured by electronically conducting electrodes is independent of whether $t_{ion} > t_e$ and, in fact, is always positive (since ΔG is negative). It is the magnitude of $\mathscr{V}_e$ that depends on whether the oxide is a good ionic or electronic conductor.

It can similarly be shown that the potential measured using electrodes that conduct ions, but not electrons, is given by (if t_e is constant)

$$\mathscr{V}_{\text{ion}}=\frac{\Delta G_{\text{MO}_\alpha}}{4e\alpha}t_e \ . \tag{2.9}$$

The electrostatic potential difference $\varphi_{\text{II}}-\varphi_{\text{I}}$ is thus seen to be of the order $\Delta G/e$, and, since $|\Delta G_{\text{MO}_\alpha}|$ is typically several electron volts, $\varphi_{\text{II}}-\varphi_{\text{I}}$ will typically be a few volts.

2. Thick film growth in terms of point defects

Wagner's theory as described in Sec. II.A.1 is a phenomenological one in which the point defect properties of the oxide are implicit in the dependence of D^* on $a(O_2)$. However, Eq. (2.3) can be applied equally well to ions or defects. It is therefore possible to use the same assumptions as in Sec. II.A.1, but to formulate the analysis in terms of point defects rather than the ions themselves (see, for example, Kröger, 1974, Chap. 23.2). As is necessary, such an approach also leads to the same eventual equations, (2.4) and (2.5). However, it is now possible within this framework to include the point defect properties explicitly in a further step. As can be seen in the following example, this approach can be more physically informative, since it is based on an atomistic picture. In this case the treatment is not strictly analogous to the Wagner theory, since it assumes local electrical neutrality rather than local chemical equilibrium within the oxide. Nevertheless, in most cases the result is the same (see Sec. II.E).

Let us consider our model oxide NiO, in which cation vacancies (V''_{Ni}) and electron holes ($\dot{h}$) can be formed by reaction with oxygen gas according to (the notation of Kröger and Vink is used for oxide defects)

$$(\text{NiO})+\tfrac{1}{2}\text{O}_2\rightarrow(\text{NiO})+\text{O}_0^{\text{x}}+V''_{\text{Ni}}+2\dot{h} \ . \tag{2.10}$$

Application of the law of mass action (chemical equilibrium) to this reaction gives

$$K_{10}=[V''_{\text{Ni}}][\dot{h}]^2/a(\text{O}_2)^{1/2} \ . \tag{2.11}$$

Square brackets denote concentrations in mole fractions. To maintain local electrical neutrality $2[V''_{\text{Ni}}]=[\dot{h}]$ and therefore $[V''_{\text{Ni}}]\propto a(\text{O}_2)^{1/6}$. Since the oxygen activities are different on the two sides of a growing film, there will be a concentration gradient of vacancies and a corresponding one of holes across the film, as depicted in Fig. 2(a). Furthermore, the concentrations at the metal/oxide interface will be much lower than at the oxide/oxygen interface, because $a(\text{O}_2)_{\text{II}}\gg a(\text{O}_2)_{\text{I}}$. Therefore, there are two equations based on Eq. (2.3), one for the flux of vacancies and another for the holes. By assuming local electrical neutrality through the film and no net electrical current across the film, one can solve the equations to give the electric field and the vacancy flux [see, for example, Atkinson (1982)]. When the holes are more mobile than the vacancies ($t_{\text{ion}}\ll 1$), the result is

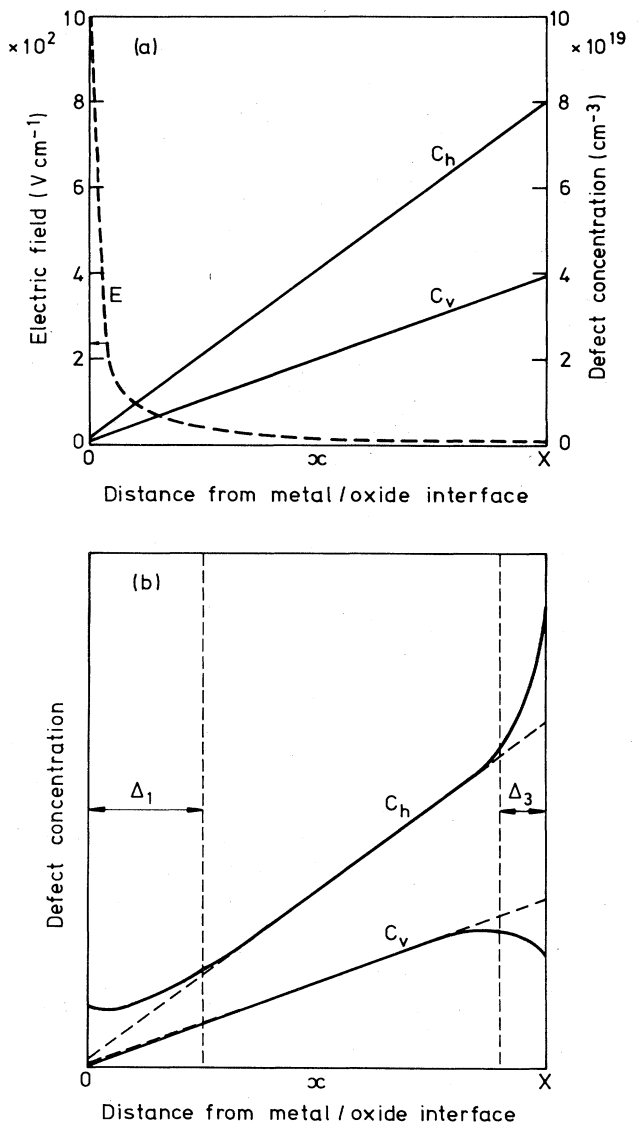

FIG. 2. (a) Concentrations of metal vacancies and holes and the electric field calculated as a function of position in a thick film of NiO growing on Ni at 1000 °C and assuming local electrical neutrality. (b) As in (a) but indicating space-charge regions near the interfaces (after Fromhold, 1979).

$$E=\frac{kT}{e}\frac{1}{[V''_{\text{Ni}}]}\frac{d[V''_{\text{Ni}}]}{dx} \tag{2.12}$$

and

$$J_v=-3D_vN_0\frac{d[V''_{\text{Ni}}]}{dx}=-3D_vN_0[V''_{\text{Ni}}]_{\text{II}}/X \ . \tag{2.13}$$

Therefore the rate of growth ($-J_v/N_0$, where N_0 is the number of oxide molecules per unit volume) is given by

$$\frac{dX}{dt}=3D_v[V''_{\text{Ni}}]_{\text{II}}/X \ . \tag{2.14}$$

Using Eq. (2.2) and noting that $D^* = D_v[V''_{Ni}]/f$, we finally have

$$k_p = \frac{6}{f} D^* , \tag{2.15}$$

where D^* is the diffusion coefficient at $a(O_2)_{II}$. This is identical to the result that would be obtained by integrating Eq. (2.5) with $D^* \propto a(O_2)^{1/6}$.

3. Expected range of validity of Wagner's theory

Wagner's theory for the growth of thick films is based essentially on assuming that bulk oxide properties and equilibria dominate the behavior. Since these assumptions become poor at sufficiently small values of film thickness, it is useful to examine the limiting thickness below which the various assumptions are unreasonable.

The Nernst-Einstein relationship, which has been used in Eq. (2.3), is valid only for small electric fields, such that $E \ll kT/ae$. However, we have seen [Eq. (2.8)] that the electric field resulting from ambipolar diffusion is of the order $100kT/eX$. Thus for the Nernst-Einstein relation to be valid we must have $X \gg 100a$, i.e., $X \gg 20$ nm.

The local chemical equilibria assumed in Wagner's theory also imply, if they are identical to bulk equilibria, that local electrical charge neutrality exists at every point within the film. This assumption is not valid close to the two interface boundaries of the film, as illustrated in Fig. 2(b). Even at equilibrium there will, in general, be a separation of charged species near an interface, resulting in a surface charge located at the interface and a space-charge region of opposite polarity extending from the interface into the film (Schottky, 1939). The extent of this space-charge region is of the order of the Debye-Hückel screening length, which is given by (Kliewer and Koehler, 1965)

$$L_D = \left[\frac{\varepsilon\varepsilon_0 kT}{e^2 C_d} \right]^{1/2} , \tag{2.16}$$

where C_d is the total number of elementary charges per unit volume resulting from charged defects (ionic and electronic) at equilibrium in the bulk oxide. The assumption of charge neutrality will be reasonable only if $X \gg L_D$. Unfortunately, it is not possible to make good estimates of L_D for many oxides because of our poor knowledge of their defect properties. Those oxides for which good data exist are those in which C_d is large and hence L_D very small. However, some crude estimates can be made by using electrical conductivity data, since $\sigma \sim C_d e u$, where u is the mobility of the charge carriers. In a typical oxide with low defect concentrations (e.g., NiO) the electronic mobility is known to be $\sim 10^{-4}$ $m^2 V^{-1} s^{-1}$ and is only weakly dependent on temperature (Tannhauser, 1974). Thus if we assume that electronic carriers in every oxide have this mobility, then C_d can be estimated from conductivity data. Debye lengths obtained in this way for some oxides are shown in Fig. 3.

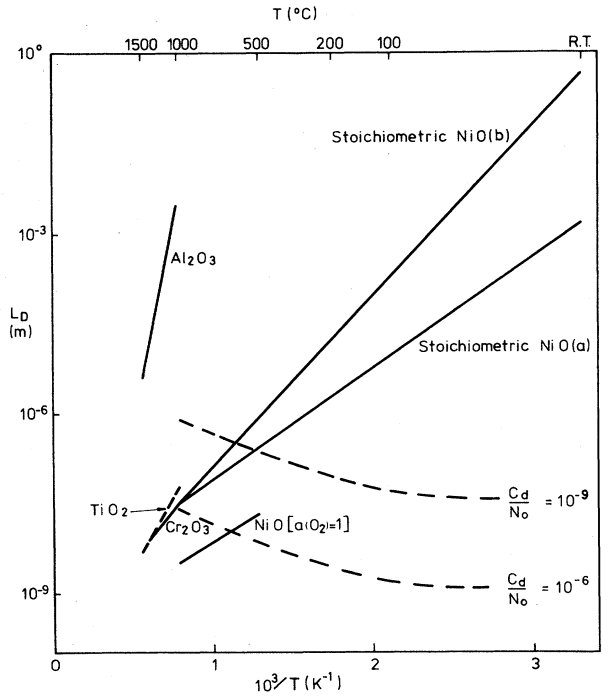

FIG. 3. Debye-Hückel screening length L_D estimated from electronic conductivity data (Kofstad, 1972) for several oxides as a function of temperature. The two sets of low-temperature data used for stoichiometric NiO are both from Wittenhauer and Van Zandt (1982). Also shown are estimates of L_D for temperature-independent charged defect concentrations of 10^{-6} and 10^{-9} per mole of MO_α.

This shows that for most oxides at temperatures above ~ 500 °C, L_D is probably less than 1 μm. However, oxides such as Al_2O_3 have very low concentrations of electronic carriers, and L_D estimated in this way is clearly too large to be sensible. In this case, L_D will be controlled by charged trace impurity defects and, for typical concentrations shown in Fig. 3, is again likely to be less than 1 μm.

There is, in addition, a further source of space charge, which is that resulting from ambipolar diffusion. There will be additional surface charges at the interfaces, giving rise to a uniform electric field in the film and also a space charge distributed through the film which arises because the ambipolar field is not uniform [Eq. (2.12)]. The space charge $\rho(x)$ at a point x within the film is related to the electrical potential by Poisson's equation

$$\frac{d^2\varphi}{dx^2} = -\frac{\rho(x)}{\varepsilon\varepsilon_0} . \tag{2.17}$$

By considering typical cases [e.g., Atkinson (1982)] we can estimate that the change in defect concentration ΔC that produces the space charge is given by

$$\frac{|\Delta C|}{C_d} \sim \frac{L_D^2}{X^2} \left[\frac{\langle C_d \rangle}{C_d} \right]^2 , \tag{2.18}$$

where C_d is the local defect concentration and $\langle C_d \rangle$ is

the average defect concentration in the film. Thus Eq. (2.18) also indicates that $X \gg L_D$ for local electrical neutrality to be a valid assumption.

We can generally conclude, therefore, that for most oxides Wagner's theory should be valid if the film thickness is greater than $\sim 1\ \mu$m for temperatures above $\sim 500\,^{\circ}$C and provided there are no barriers to the attainment of local equilibrium. In oxides with large concentrations of charged defects ($L_D \lesssim 20$ nm), the fact that the Nernst-Einstein relationship is valid only for small fields means that Wagner's theory is valid only for films greater than about 20 nm in thickness. In oxides with smaller concentrations of charged defects it is L_D which determines the lower bound of film thickness for which the theory is valid. Caution should be exercised in extrapolation to low temperatures, since very little is known about the defect structure of films grown under such conditions.

B. Theory of thin film growth

When the films are less than $\sim 1\ \mu$m in thickness, the concept of electrical neutrality within the film is unreliable, and when less than ~ 20 nm, the Nernst-Einstein relationship is no longer appropriate. Thus theories of thin film growth must consider atom jumps in the presence of large electric fields and the possibility of large space charges. There have been several approaches to film formation under these conditions, and these have been reviewed by Lawless (1974) and Smeltzer and Young (1975). Since there appears to be no consensus on what assumptions are reasonable for thin films, there are several theories and a corresponding number of kinetic expressions for thin film growth—logarithmic, inverse logarithmic, cubic, parabolic, etc.

The theory of Cabrera and Mott (1949) is useful to consider in some detail since it is not only based on assumptions which are diametrically opposed to those of Wagner but also because it describes the oxidation in atomistic rather than phenomenological terms. The first assumption made in the theory is that electrons can freely pass from the metal to ionize adsorbed oxygen atoms or molecules at the oxide/gas interface, so that the electron electrochemical potential (Fermi level) is equal in the metal and the adsorbed layer. There is thus a uniform field in the film (zero space charge) created by a positive surface charge on the metal and a negative one from excess oxygen ions (we shall assume them to be O^{2-} ions) on the oxide/gas interface. The single-electron energy levels before and after the initial transfer of electrons are shown in Fig. 4. In the Cabrera and Mott mechanism of oxidation it is the field created by this electron transfer that drives the slow ionic transport across the film and causes it to thicken. The electrons continue to cross the film readily to maintain zero electrical current.

We must now consider how the electrons pass through the film, the magnitudes of potential difference and surface charge density, and eventually the oxidation rate. The transport of electrons by tunneling and thermionic emission has been considered in detail by Fromhold and co-workers (see Sec. II.E). The result is that the assumption of electronic equilibrium is expected to be reasonable for all very thin (tunneling) films and, in some cases, for thicker films, depending on the band structure of the oxide.

To analyze the charges, voltage, and growth rate we shall follow the extension of the basic theory due to Grimley (1955). The basis of this approach is to assume that the adsorbed layer of ions is in equilibrium with the gas and to recognize that this same layer provides the surface charge and the voltage across the film $\Delta\varphi$. The electron transfer and adsorption reaction can be written as a

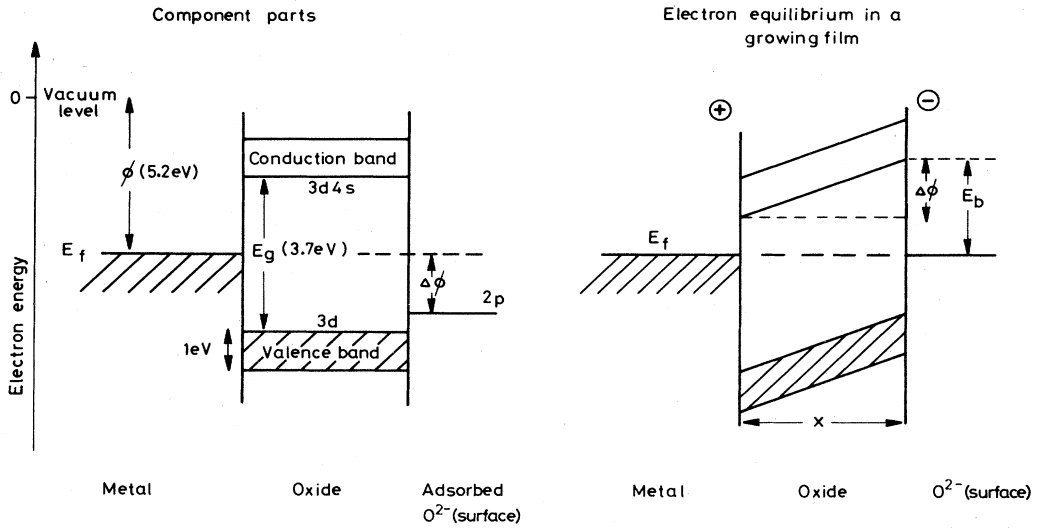

FIG. 4. Electron energy-level diagrams illustrating how, in the theory of Cabrera and Mott (1949), the ready transfer of electrons from the metal to oxygen adsorbed on the surface of a thin, growing oxide film generates a uniform electric field. The energies and band labels are for Ni and NiO.

reaction of the type

$$\tfrac{1}{2}O_2(\text{gas})+2e(\text{metal})\rightarrow O^{2-}(\text{surface}) . \quad (2.19)$$

This is the simplest surface reaction but not necessarily the correct one, since other surface species, either charged (O^-, O_2^-) or uncharged (O_2, O), may also be involved (see Sec. II.E). We treat only the simplest case here, but recognize that it can be extended to more complicated surface equilibria.

Since reaction (2.19) is assumed to be in equilibrium, we can make use of its equilibrium constant

$$K_{19}=\frac{a(O^{2-})}{a(O_2)^{1/2}a(e)^2} , \quad (2.20)$$

where K_{19} is related to the standard free-energy change of equation (2.19) in the usual way [$K_{19}=\exp(-\Delta G^\circ_{19}/kT)$]. If the surface coverage of excess O^{2-} ions is low, then $a(O^{2-})=n_0/N_s$, where n_0 is the number of excess O^{2-} ions and N_s the total number of O^{2-} ions in unit area of the surface. $a(e)$ is the activity of an electron with respect to the Fermi energy of the metal and is equal to $\exp(-e\Delta\varphi/kT)$. (N.B. The electrochemical potential $\mu-e\varphi$ is constant and $\Delta\varphi$ is a positive quantity.) Therefore, we have the following relationship between n_0 and $\Delta\varphi$:

$$n_0=N_s a(O_2)^{1/2}\exp[-(\Delta G^\circ_{19}+2e\Delta\varphi)/kT] . \quad (2.21)$$

Since the film and surface charges may be regarded as a simple capacitor, we also have

$$n_0=\frac{\varepsilon\varepsilon_0\Delta\varphi}{2eX} . \quad (2.22)$$

Solving Eqs. (2.19) and (2.22) for $\Delta\varphi$, we obtain

$$\frac{2e\Delta\varphi}{kT}+\ln\left[\frac{2e\Delta\varphi}{kT}\right]=-\frac{\Delta G^\circ_{19}}{kT}+\ln\left[\frac{4e^2N_s a(O_2)^{1/2}X}{kT\varepsilon\varepsilon_0}\right] . \quad (2.23)$$

Since normally $e\Delta\varphi/kT\gg 1$, then the second term on the left-hand side is negligible and hence

$$\Delta\varphi\simeq-\frac{\Delta G^\circ_{19}}{2e}+\frac{kT}{2e}\ln\left[\frac{4e^2N_s a(O_2)^{1/2}X}{kT\varepsilon\varepsilon_0}\right] . \quad (2.24)$$

From this equation we deduce that $\Delta\varphi$ is related mainly to the free-energy change of reaction (2.19) (cf. Fig. 4) but is also dependent on T and, more weakly, on $a(O_2)$ and X.

The surface excess of oxygen ions can now be calculated from Eq. (2.22). For $\Delta\varphi=1$ V, $\epsilon=10$, and $X=10$ nm, $n_0=2.8\times10^{16}$ m^{-2}, which is a small fraction of a monolayer.

To calculate the oxidation rate Cabrera and Mott assumed that the rate-controlling process is the injection of a defect into the oxide at one of the film interfaces. Since the treatment is slightly different, depending on which interface is injecting the defect, it is appropriate to consider the two cases separately.

1. Oxide defects injected at the metal/oxide interface

This is the simplest case, and the defect could be an oxygen vacancy, or an interstitial metal ion. We shall examine the latter example injected by the reaction [Fig. 5(a)]

$$M(\text{metal})\rightarrow M_i^{\cdot\cdot}(\text{oxide})+2e(\text{metal})+V(\text{metal}) . \quad (2.25)$$

The potential energy of the metal atom as it moves from the metal into the oxide across the interface (and becomes ionized) is shown schematically in Fig. 6. The activation energy for the jump from the metal into the film (W) is greater than the activation energy for its subsequent jumps through the film (ΔH_m), and $W-\Delta H_m$ is the energy of incorporation of the defect, i.e., the energy change of reaction (2.25). Under the influence of the electric field developed during film growth the barriers for the interface and oxide jumps to the right are reduced, as shown in Fig. 6, by an amount $qa\Delta\varphi/2X$. In the Wagner treatment of oxidation such an interface is assumed to be in equilibrium, requiring that the frequency of jumps to the right through the saddle point S_0 be approximately equal to the frequency of jumps in the opposite direction. Cabrera and Mott, on the other hand, consider this interface to be far from equilibrium, because if the field is large enough the jumps are biased overwhelmingly to the right. The condition for the reverse jumps to be negligible is $\frac{1}{2}qaE\gg kT$. This is the same condition for the Nernst-Einstein relation to be invalid (see Sec. II.A.3) and is likely to be true for films less than 20 nm in thickness. Since the interface jump has the highest activation energy, the rate of such jumps determines the rate of film growth. In the high-field limit, which is necessary for the interface to be far from equilibrium, the jump rate corresponds

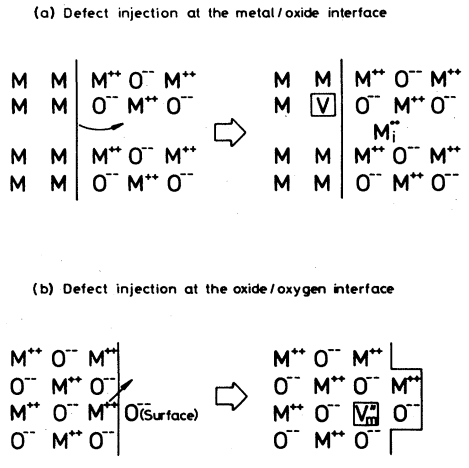

FIG. 5. An illustration of possible reactions for the injection of point defects into the oxide film by (a) the transfer of a metal atom to an interstitial oxide site at the metal/oxide interface, (b) the transfer of a metal ion to a site next to an oxygen ion on the oxide/oxygen interface to create a metal vacancy in the oxide.

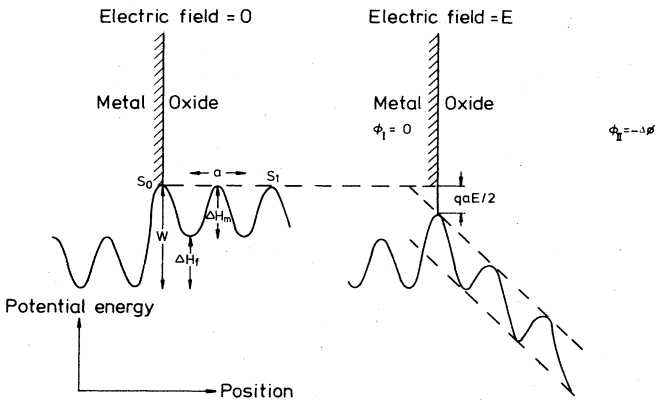

FIG. 6. Schematic diagrams (after Cabrera and Mott, 1949) showing the potential energy of an interstitial metal "ion" as a function of position near the metal/oxide interface during thin film growth. The electrical field generated by the transfer of electrons from metal to oxygen lowers the energy barriers for ions moving away from the metal/oxide interface.

to a growth rate given by

$$\frac{dX}{dt}=a\nu\exp(-W/kT)\exp\left[\frac{qa\Delta\varphi}{2kTX}\right], \tag{2.26}$$

where ν is the vibrational frequency of the atoms at the interface. This may be conveniently written in the form

$$\frac{dX}{dt}=\frac{D_i}{a}\exp\left[\frac{X_1}{X}\right], \tag{2.27}$$

where $X_1=qa\Delta\varphi/2kT$, and is equal to the upper limit of thickness for validity of the basic assumptions, and $D_i=a^2\nu\exp(-W/kT)$ and has the dimensions of a diffusion coefficient. If we further assume that the energy at the saddle point of the interface jump (S_0) is the same as that for subsequent jumps through the oxide, then W can be related to the activation energy for diffusion in the oxide (see Sec. II.C.2). Equation (2.27) predicts an oxidation rate that decreases exponentially as the thickness increases. When $X \ll X_1$, Eq. (2.7) can be integrated approximately to give the inverse logarithmic kinetic equation

$$\frac{X_1}{X}\simeq-\ln\left[\frac{D_iX_1t}{aX_L^2}\right]. \tag{2.28}$$

X_L has the significance of a limiting thickness above which the growth rate falls below some arbitrary negligible value. According to Cabrera and Mott's criterion of a negligible rate (10^{-15} ms^{-1}), X_L is given by

$$X_L\simeq X_1\Big/\left[\frac{W}{kT}-39\right]. \tag{2.29}$$

Since X_1 is the upper limit for validity of the theory, the temperature $W/40k$ (when $X_L=X_1$) is a critical temperature. When $T<W/40k$ the film grows to a limiting thickness X_L ($<X_1$), but when $T>W/40k$ the film continues to grow past X_1 and eventually into the parabolic regime.

Ghez (1973) pointed out that the mathematical approximations leading to Eq. (2.28) are sufficiently poor as to make the inverse logarithmic kinetics so predicted a poor test of the Cabrera and Mott theory. Better tests are to plot $\ln(dX/dt)$ against $1/X$ [from Eq. (2.27)], or $\ln(t/X^2)$ against $1/X$ as suggested by Ghez.

2. Oxide defects injected at the oxide/gas interface

When the defect is injected into the oxide at the oxide/gas interface, the defect could be an oxygen interstitial or metal vacancy. Using the latter as an example, we can write the injection reaction [all oxide sites, Fig. 5(b)]

$$M_M^x+O^{2-}(\text{surface})\rightarrow V_M''+MO\ . \tag{2.30}$$

Calculation of the oxidation rate controlled by this reaction proceeds as for the case of injection at the other interface, but with one difference. This is that only those metal ions that can reach an O^{2-}(surface) ion in one jump can participate in reaction (2.30). The number per O^{2-}(surface) ion will depend on the geometrical arrangement of atoms around the surface ion. On the average, it will be a number close to 5. The growth rate therefore depends on the concentration of O^{2-}(surface) ions. The resulting expression for the growth rate analogous to Eq. (2.26) is

$$\frac{dX}{dt}=5a\nu\frac{n_0}{N_s}\exp\left[\frac{-W}{kT}\right]\exp\left[\frac{qa\Delta\varphi}{2kTX}\right]. \tag{2.31}$$

If we use Eq. (2.22) for n_0, the expression for the growth rate analogous to Eq. (2.27) is

$$\frac{dX}{dt}=\left[\frac{5\varepsilon\varepsilon_0\Delta\varphi}{2eN_sX}\right]\frac{D_i}{a}\exp\left[\frac{X_1}{X}\right]. \tag{2.32}$$

This equation predicts slightly different kinetics from Eq. (2.27) because of the appearance of X in the denominator.

When X is 10 nm, the first term in large parentheses is $\sim10^{-2}$. This leads to a smaller limiting thickness of oxide than predicted for injection at the metal/oxide interface. The expression analogous to Eq. (2.29) for the limiting thickness is

$$X_L\simeq X_1\Big/\left[\frac{W}{kT}-39+\ln X_L(\text{nm})\right], \tag{2.33}$$

and the critical temperature remains approximately unchanged.

C. Comparing theory with experiment

Ideally, whether for thick or thin films, one would wish to test all the theoretical predictions by experimental ob-

servations. The following theoretical predictions should be verifiable, in principle:

(a) the growth rate as a function of time,
(b) the growth rate as a function of oxygen activity,
(c) the magnitude of the growth rate in terms of independently measurable parameters, and
(d) the magnitude of the electric field in the growing film.

In addition, there are other experiments that can be done to probe the mechanism. The two which have been used most are

(e) the response to an externally applied electric field, and
(f) the migration of tracer atoms in the growing film.

We shall consider topics (a)—(e) with reference to thick films and then to thin films. Since the information from tracers is not so dependent on film thickness, this topic will be considered separately.

1. Thick films (Wagner)

The growth kinetics predicted by Wagner's theory are parabolic. In many cases it is found experimentally that there are significant deviations from exact parabolic kinetics. In the past there has been a tendency to overinterpret these deviations in terms of different growth mechanisms. This has proved to be unreliable, because small perturbations of the basic mechanism (e.g., gradual loss of contact at the metal/oxide interface) can be responsible for such deviations from ideal behavior.

The functional dependence of k_p on $a(O_2)$ can be calculated from Eq. (2.5). In general when defects are injected into the oxide at the metal/oxide interface (O vacancies or M interstitials), k_p is independent of $a(O_2)$, and when injection takes place at the oxide/gas interface (O interstitials or M vacancies), k_p has the same dependence on $a(O_2)$ as does the tracer diffusion coefficient [usually $a(O_2)^n$]. The magnitude of k_p also may be calculated from Eq. (2.5) if the tracer diffusion coefficient of the more mobile ions is known as a function of $a(O_2)$. The approximate result is that k_p is of the same order as the maximum value of D^*.

As described in Sec. II.A, the electric field within the oxide is not directly measurable by external probes. When the metal/oxide and oxide/gas interfaces are probed with electronically conducting electrodes, the magnitude of the voltage enables the mean ionic transport number of the oxide to be deduced from Eq. (2.8).

However, this enables a conclusion to be drawn concerning only the relative magnitudes of ionic and electronic conductivities and not the relative fluxes of charged and uncharged species. Thus a film growing mainly by the transport of uncharged species could still show an open circuit voltage due to the minority-charged species, provided that their currents were sufficiently high to satisfy the currents drawn by the measuring instruments (see, for example, the controversy regarding charged species in SiO_2 growth).

When the film is contacted using such an electrode, the growth process can be influenced by conditions in the external circuit between the electrode and the metal substrate. If the external circuit is short-circuited, then electrons can pass freely from the metal substrate to the oxide/gas interface. The result is always that the growth rate of the film is increased. Since the external circuit is an electronic short circuit, the new growth rate can be obtained from the usual film-growth equations by artificially assuming electronic conductivity dominates in the oxide—i.e., the rate is multiplied by a factor $1/t_e$. Therefore, the increase is negligible if the oxide is already a good electronic conductor, but may be large if ionic conductivity is dominant. If a potential is imposed by a voltage generator in the external circuit ($\mathscr{V}_{\rm ext}$ with respect to the metal substrate), this fixes the electrochemical potential difference of electrons across the film, i.e., $\eta_{\rm II}-\eta_{\rm I}=-e\mathscr{V}_{\rm ext}$, as in Eqs. (2.6) and (2.7). It is therefore apparent that when $\mathscr{V}_{\rm ext}$ is positive, and is equal to the $\mathscr{V}_e$ given by Eq. (2.8), the external current has no effect on the growth rate. Since $\mathscr{V}_e$ is always positive, a negative applied $\mathscr{V}_{\rm ext}$ will always increase the growth rate to a value which exceeds even the short-circuit growth rate ($\mathscr{V}_{\rm ext}=0$). When $\mathscr{V}_{\rm ext}$ is positive and is greater than $\mathscr{V}_e$, the growth rate is slowed down until the growth stops completely at an external voltage $\mathscr{V}_{\rm stop}$ given by (Kröger, 1974, Chap. 23.2.5):

$$\mathscr{V}_{\rm stop}=-\frac{\Delta G_{\rm MO_\alpha}}{2e\alpha}=\frac{\mathscr{V}_e}{t_{\rm ion}}\ , \tag{2.34}$$

when the ionic defects have conventional charges. If $\mathscr{V}_{\rm ext}>\mathscr{V}_{\rm stop}$, then the growth rate becomes negative and the film is decomposed by electrolysis.

Therefore, experiments with externally applied voltages do not give any information beyond that given by a measurement of the open circuit voltage—i.e., $t_{\rm ion}$ is determined. However, if Eq. (2.34) is found to be obeyed, then the growth is shown to be an ionic process with interfaces in local equilibrium.

2. Thin films (Cabrera and Mott)

Comparison between theory and experiment is much more difficult for thin films than for thick films. The kinetic equations are more complicated, and the oftenquoted inverse logarithmic law is only an approximation (and then only when defects are injected into the oxide at the metal/oxide interface). Therefore, the observation that some data fit direct logarithmic kinetics better than they do inverse logarithmic ones cannot be interpreted as showing the basic mechanism to be invalid. By the same argument, it would be unreliable to attempt to distinguish between defect injection at the metal/oxide and oxide/gas

interfaces on the grounds of their slightly different predicted kinetics.

The dependence of growth rate on $a(O_2)$ at a given film thickness may also, in principle, be used to make such a distinction. However, in both cases dX/dt is only weakly dependent on $a(O_2)$, and the difference between them would be difficult to resolve. The effect on thin-film growth of an external potential, $\mathscr{V}_{ext}$ (with respect to the substrate), applied using metallic electrodes is given by simply replacing $\Delta\varphi$ by $\Delta\varphi - \mathscr{V}_{ext}$ in Eqs. (2.21), (2.26), and (2.31). Thus making the oxide/gas interface negative increases the growth rate and vice versa.

When a quantitative prediction of the growth rate is sought, the Cabrera and Mott mechanism is particularly difficult to apply. This is because the free-energy changes and activation energies for the defect injection and gas adsorption reactions are not known through independent means. At best they can be estimated from theoretical treatments or by making further approximations. This is probably best illustrated by the use of an example. For this purpose we will attempt to apply the theory to the growth of NiO (our model oxide) at 500 °C and $a(O_2)=1$. Since this oxide is known to contain cation vacancies, the discussion of Sec. II.B.2 is the appropriate one. We first require the free-energy change of reaction (2.19) in order to calculate the voltage $\Delta\varphi$. The enthalpy change contributing to ΔG°_{19} can be estimated from the component parts of the reaction

$$\Delta H^\circ_{19} = 2\varphi_M + \tfrac{1}{2}\Delta H_D + \chi_2 - \tfrac{1}{2}E_c \ . \qquad (2.35)$$

In this expression φ_M is the nickel work function (5.2 eV), ΔH_D the energy to dissociate the O_2 molecule (5.08 eV), χ_2 the second electron affinity of oxygen (7.8 eV), and E_c the cohesive energy of NiO (41.8 eV). Thus $\Delta H^\circ_{19}=0.16$ eV. The entropy of O_2 gas is $\sim 2\times 10^{-3}$ eV K^{-1} and therefore at 500 °C $\Delta G^\circ_{19}\simeq 0.61$ eV. Substituting into Eq. (2.24), we find that $\Delta\varphi$ is predicted to be negative, whereas it should be positive. It is therefore evident that either the uncertainties in the calculation of $\Delta\varphi$ are too great for an estimate to be reliable, or Eq. (2.19) is oversimplistic. The next parameter that is required is the energy change of the injection reaction [Eq. (2.30)]. Again, this is a parameter which is not measurable in bulk NiO, because the Ni vacancy is accompanied by two holes in the bulk [Eq. (2.10)]. We are thus driven again to use theoretical estimates. The energy required to remove a Ni ion from NiO to infinity has been calculated by Sangster and Rowell (1981) and Catlow *et al.* (1979). The mean of the two estimates is 24.0±0.5 eV. To find the energy for the injection reaction we must subtract $\frac{1}{2}E_c$ for the reincorporation of the ion onto the surface. Hence $W-\Delta H_m$ is estimated to be 3.1 eV. ΔH_m can be measured by experiments on bulk material, and the best estimate is 1.58 eV (Atkinson *et al.*, 1981). Therefore, W is estimated to be 4.7 eV, with a probable error of at least 0.5 eV. It can readily be seen that this estimate is far too large to be realistic. It implies a critical temperature ($W/40k$, below which a limiting thickness is reached) of 1090 °C, but at this temperature Wagner's theory predicts a measurable growth rate based on bulk diffusion. We are thus forced to conclude that it is not possible to subject the Cabrera and Mott theory to a rigorous quantitative test. Probably the best that can be done is to make some sweeping approximations to obtain more realistic (but not necessarily

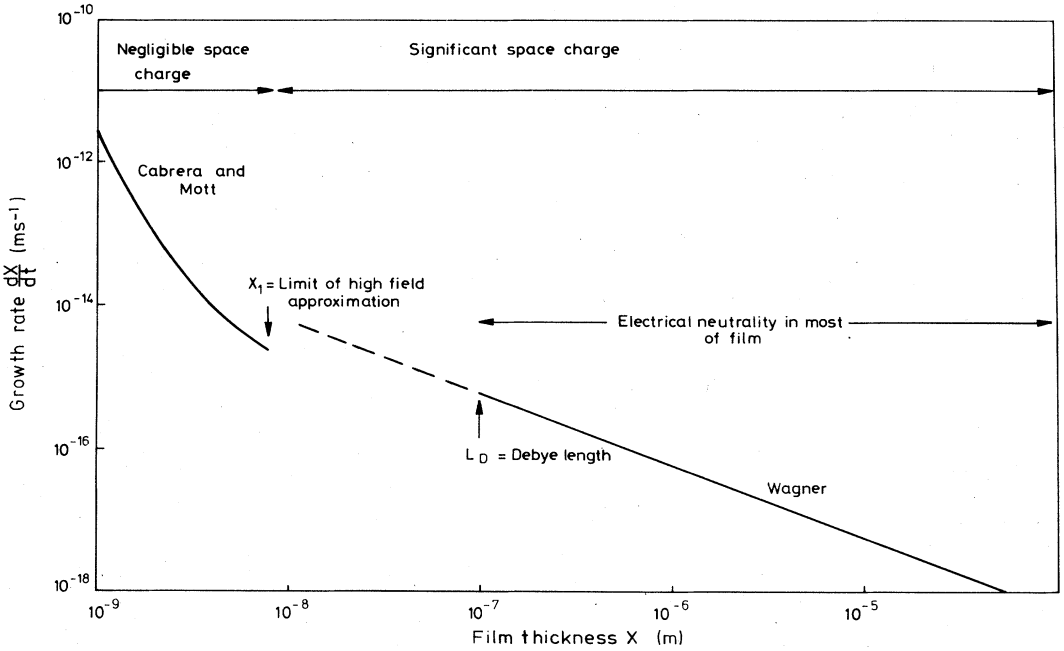

FIG. 7. Rate of growth of a hypothetical p-type oxide film as a function of its thickness, calculated using the theory of Cabrera and Mott when thin ($X < X_1$) and of Wagner when thick ($X > L_D$ and X_1). The parameters used are appropriate to a film of NiO growing by lattice diffusion at 500 °C.

correct) estimates. Suitable approximate estimates would be the free energy of formation of the oxide per oxygen atom [i.e., $(1/\alpha)\Delta G^{\circ}_{MO_\alpha}$] for ΔG°_{19} and the activation energy of the tracer diffusion coefficient in the oxide [at constant $a(O_2)$] for W. Using these approximations for NiO, we have $\Delta G^{\circ}_{19} = -1.7$ eV and $W = 2.56$ eV.

These values have been used to calculate dX/dt as a function of X for NiO growing on Ni at 500 °C, and the result is shown in Fig. 7. Also shown is that calculated from the lattice diffusion coefficient (Atkinson and Taylor, 1981) using Wagner's theory in the thick film region. At the limits of validity of the two theories the predicted growth rates are mutually compatible. This would indicate that the approximate estimates for ΔG°_{19} and W are reasonable.

D. Atom tracers in growing films

Experiments using tracer atoms while the film is growing have proved particularly useful in identifying which species are the more mobile and the pathways by which they are transported. This is because the interpretation of such experiments, at least in qualitative terms, is independent of the kinetic regime of growth. There are two basic experiments of this type, one with labeled metal atoms and the other with labeled oxygen atoms.

The experiment involving metal atoms consists of labeling the surface atoms of the metal by deposition of radiotracer atoms prior to oxidation. After oxidation the film is sectioned to determine the concentration of tracer as a function of depth in the film. The resulting distribution is a function of whether metal or oxygen is the more mobile in the film and of whether the metal transport is through the oxide lattice or along short-circuit paths such as grain boundaries or dislocations (Atkinson *et al.*, 1979). However, the short-circuit transport can be distinguished from the bulk only if $(D^*t)^{1/2} < l$, where l is the distance between the short-circuit paths (e.g., the grain size). If this condition is not satisfied, the atoms in the short-circuit paths will have mixed with those in the lattice, and the result will be indistinguishable from lattice diffusion. In principle, this experiment can, in the case of lattice diffusion, differentiate between diffusion via vacancies and interstitials (Atkinson and Taylor, 1982) and can also indicate the charge on the defect. However, in practice such subtleties are beyond the precision of the experimental techniques. The distributions resulting from various transport processes are summarized in Fig. 8.

When oxygen tracers are used, the experiment normally consists of first growing a film in oxygen of normal isotopic composition (99.759% ^{16}O) followed by subsequent growth in an atmosphere enriched in ^{18}O. The distribution of ^{18}O in the film is finally measured either by secondary-ion mass spectroscopy (SIMS) or by a nuclear technique. The ^{18}O tracer may have been incorporated into the film either by the formation of new oxide (in which case the location of the reaction is revealed) or by exchange with ^{16}O in the first-grown film. Mitchell *et al.* (1983) have recently described how these two methods of incorporation can be distinguished in SIMS. The distinction is based on the fact that exchange is the main process which results in mixed species of the type $M^{18}O^{16}O^-$ appearing in the SIMS spectrum. The technique requires that the second stage of the oxidation be carried out in $^{18}O_2$ containing a minimum of $^{16}O_2$; otherwise, mixing can occur in the gas as well as by exchange in the solid.

The ^{18}O profiles in films grown sequentially in $^{16}O_2/^{18}O_2$ are shown schematically in Fig. 8. They can in principle be used to distinguish between oxygen and metal transport and, in the case of oxygen, between lattice and short-circuit diffusion. The combination of both metal and oxygen tracer experiments is therefore very useful in

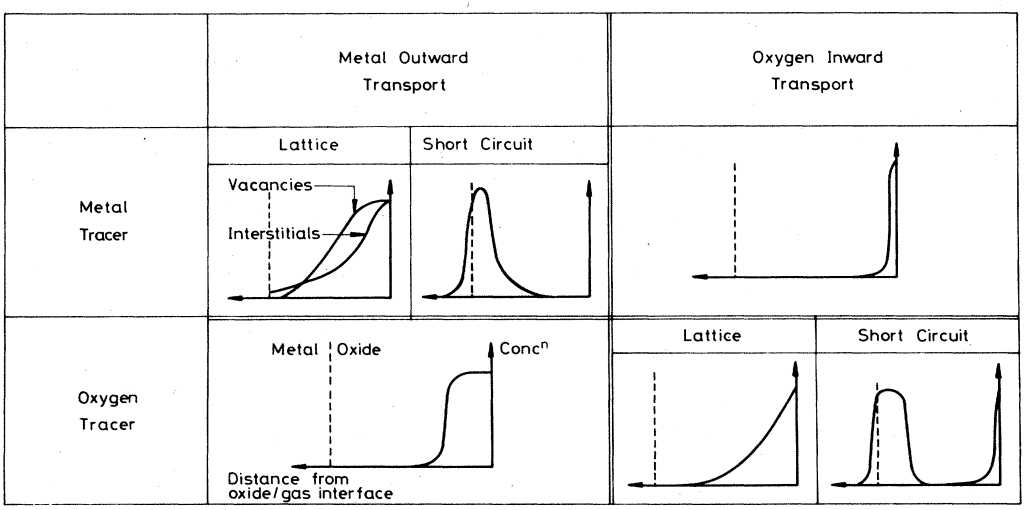

FIG. 8. Distributions of tracer atoms expected in oxide films growing by different transport processes. In the experiment with metal tracer, a thin film of tracer is deposited on the metal prior to film growth. In the experiment with oxygen tracer, the film is grown sequentially, first in ^{16}O- and then in ^{18}O-labeled gas.

identifying the dominant transport processes in the growing film.

E. Less restrictive theories of film growth

The theories of Wagner, for thick films, and of Cabrera and Mott, for thin films, are based on assumptions which are likely to be valid only in the extremes of very thick and very thin films, respectively. Some rough estimate of the limits of applicability of these theories can be made based on the guidelines given in earlier sections. Compatibility with these limitations, although necessary, is not a sufficient condition for the theories to be valid. For example, the condition that $X < X_1$ [Eq. (2.27)] for application of the Cabrera and Mott theory ensures only that the high-field approximation for ionic transport is valid. It does not ensure that electrons can be transferred to adsorbed oxygen in order to create the high electric field. If an approach to film growth were to be completely general, it would have to include the dynamics and energetics of processes at the interfaces, coupled transport of both ions and electrons in high and low fields by all possible routes, surface charges at the interfaces, and space charges within the film, etc. (Even this does not include the initial nucleation of the oxide film.) The relevant equations describing these phenomena and how they may be coupled in the overall growth process are concisely summarized in the review of Smeltzer and Young (1975) and will not be reiterated here. It is sufficient to note that the overall process is potentially so complex that it may be tackled only by making different degrees of approximation. Here I mention briefly some theoretical treatments of film growth which have been less restrictive in their assumptions than those of Wagner and Cabrera and Mott. It is evident from the illustrative example shown in Fig. 7 that in general there is an intermediate region of film thickness, approximately between X_1 and L_D, in which even the basic assumptions of the simpler theories are invalid, in that the film is too thick for the high-field approximation and too thin to be considered as predominantly electrically neutral. Less restrictive theories are necessary for describing the growth of thin films into thick films through this intermediate region.

The most general theoretical approach to transport processes within the growing film has been taken by Fromhold and co-workers who have attempted to cover all regions of film thickness while keeping the number of simplifying assumptions to a minimum. The basic underlying principle is to achieve a steady-state distribution of electronic and ionic defects which satisfy Poisson's equation and give equal, and nondivergent, electronic and ionic currents. Unfortunately, the resulting equations can be solved only by numerical means, and the reader is referred to Fromhold (1976,1980) for a detailed treatment and references to the original papers.

This approach has been used to examine the efficiency of tunneling and thermionic emission as electronic transport mechanisms in thin film growth. The calculations demonstrate (Fromhold, 1976, Chap. 10) that tunneling through the oxide can only give a sufficiently large current for films less than about 3 nm in thickness. For such films the computed growth kinetics are in good agreement with the simplified theory of Cabrera and Mott, but for films thicker than about 3 nm the electron tunnel current becomes so low as to be rate limiting, provided there is no alternative pathway for the electrons. Direct thermonic emission (of electrons via the oxide conduction band, or holes via the valence band) has been similarly examined (Fromhold, 1976, Chap. 11) as an alternative electronic transport process for films thinner than the mean free path of electronic carriers in the oxide (this is an unknown quantity, but is unlikely to be greater than about 30 nm). Calculations demonstrate that when electrons are transported by thermionic emission, either electron transport or ion transport can control film growth, depending on the relative positions of the electron energy levels in metal, oxide and adsorbed oxygen, and the activation energy for ionic motion. In general, ionic motion limits the rate of film growth when the ionic activation energy (W in Fig. 6) is greater (by at least 0.2 eV) than the effective work function for electron emission into the oxide from the metal (or hole emission from adsorbed oxygen). Under these conditions the electron system is in "virtual equilibrium." The electron energy levels tend to equilibrate as depicted schematically in Fig. 4 (with E_b being the approximate barrier height for electron emission), but the potential difference across the growing film is slightly different from that in the Cabrera and Mott theory. (When electron emission is rate limiting, the potential difference is in the opposite sense.) The computed film-growth kinetics approximate those of the Cabrera and Mott model in the limit of high fields and take on parabolic form at low fields. The corresponding parabolic rate constant is not the same as that of the thick film theory of Wagner, since the thin film is not electrically neutral locally and the electric field is assumed to be uniform.

As a film thickens, the total charge associated with defects moving through the film (space charge) will eventually exceed that on the film boundaries and the field will not be uniform. Numerical studies of these perturbations (Fromhold, 1976, Chap. 12), using a model in which the defect concentrations are fixed at the film interfaces, demonstrate that as the film thickens the defect distributions tend towards establishing electrical neutrality within the film. Ultimately the film may be divided into three regions, as depicted in Fig. 2(b). The central region is effectively electrically neutral, while the zones near the interfaces are not and extend for a distance of the order of the local Debye-Hückel screening length L_D from each interface. The analysis of this situation (Fromhold, 1979) is similar to that of the point defect description of thick film growth given in Sec. II.A.2 and predicts parabolic growth kinetics. The resulting parabolic rate constant is not strictly the same as that of the Wagner theory, since local chemical equilibrium has not been assumed in this case, nor has electrical neutrality been assumed in Wagner's theory. There is, however, no practically useful

distinction between these rate constants, because the eventual evaluation of the rate constant in Wagner's theory, in terms of bulk equilibrium properties, implicitly incorporates electrical neutrality.

The extensive treatments of Fromhold and co-workers have shown that when transport of one species (e.g., ions) is so slow as to be rate controlling, the more readily transported species (e.g., electrons) approach an equilibrium distribution. The simplifications that result from such a "virtual electronic equilibrium" have been exploited by Dignam, Young, and Goad (1973) and Young and Dignam (1973). They noted that measurements of the electronic conductivity of many oxide films indicate that their interfaces are ohmic (i.e., without substantial barriers to carrier transfer) and that the conductivities are sufficiently high to maintain the "virtual electronic equilibrium." This they attribute to the existence of short-circuit transport paths for electrons in the film (e.g., grain boundaries). Within this approximation they extended the theory of Cabrera and Mott to include a range of possible equilibria at the oxide/oxygen interace (see Sec. II.B, for example), injection of ionic defects into the film and their field-assisted transport through the film in the associated space-charge field. The equation that was used to describe the ionic current density is valid at both high and low fields, but does not include diffusion (i.e., transport resulting from a defect concentration gradient). Therefore, the analysis may be applied to films growing up to and beyond the high-field limit (X_1) but not into the thick-film region where contributions from diffusion and drift in the electric field are approximately equal. When space-charge effects are neglected, analytical equations for film growth are obtained under some limiting conditions. The trend is to give logarithmic-type kinetics in the high-field limit and, in the low-field limit, parabolic kinetics when defects are injected at the metal/oxide interface and cubic kinetics when injected at the oxide/gas interface. The rate equations, dependence on oxygen activity, and the activation energy for growth are tabulated in Young and Dignam (1973) for the various limiting cases. When space charges are included, the equations can be solved only numerically.

It may be concluded that much of the methodology exists to describe the growth of an oxide film over the entire thickness range. As far as the author is aware, such a description has never been attempted using a single set of atomistic parameters derived either from other experiments or by calculation (see Sec. II.C.2). This would appear to be one way of developing a more comprehensive view of film growth, since it is clear that the fitting of experimental data to theoretical kinetics, whether analytical or numerical, is an inadequate test of theory (Smeltzer and Young, 1975).

III. GROWTH OF SOME SELECTED OXIDES

In this section the growth of some specific oxides is discussed in terms of the concepts presented in Sec. II. The oxides have been chosen either because they have proved useful as model oxides or because they are important as corrosion resistant oxides.

The first oxide to be considered is CoO, because both the growth kinetics and diffusion data are well established for this oxide. It therefore provides a good test of Wagner's theory for thick-film growth. However, it is not a good model of a corrosion resistant oxide for two reasons. The first is that the growth of an overlayer of Co_3O_4 complicates the reaction at temperatures below 950 °C. Secondly, and more importantly, the growth rate at temperatures above 950 °C is extremely rapid because of the high concentration of point defects in CoO. Hence the growth rates are not representative of those of corrosion-resistant oxides.

NiO is far more appropriate as a model for a corrosion-resistant oxide. It is also convenient in that NiO is the only oxide which grows by the thermal oxidation of Ni and can therefore be studied over a very wide temperature range (up to the melting point of Ni). Consequently, the growth of this oxide has deservedly received much attention and that is reflected in this paper.

The growth of iron oxides is then discussed, because it introduces the complexity of films that contain more than one oxide and because the corrosion rate of low-alloy steels is controlled by the rate of growth of iron oxides.

Finally, we consider the growth of Cr_2O_3 and Al_2O_3 films because of their importance in conferring very good corrosion resistance at relatively high temperatures. Unfortunately, the very low point defect concentrations, which are ultimately responsible for this good corrosion resistance, make studies of these oxides very difficult.

A. Growth of CoO

The high-temperature properties of bulk CoO are well understood (e.g., Kofstad, 1972). It is a p-type electronic conductor and is metal deficient. The cation vacancy concentration increases with oxygen activity by a reaction similar to Eq. (2.10) to $\sim 6\times 10^{-3}$ mole fraction at 1 atm and 1000 °C. The Co diffusivity is several orders of magnitude greater than that of oxygen (Chen and Jackson, 1969). Cobalt diffusion measurements show good agreement between different workers, and the more recent studies of Dieckmann (1977) and Peterson and Chen (1980) show that at 1200 °C diffusion is by singly charged cation vacancies at high oxygen activity and doubly charged vacancies at low oxygen activity. There seems to be no evidence of more complex defect aggregates despite the relatively high defect concentration. The cation diffusion coefficients for CoO and some similar oxides are shown as a function of $a(O_2)$ in Fig. 9.

The majority of oxidation studies have been at these high temperatures and firmly in the region of thick film growth where Wagner's theory should be valid. This system, therefore, is an excellent one for a rigorous test of the theory. Since the tracer diffusion measurements show that $D^* \propto a(O_2)^{1/4}$ at high oxygen pressures, Eq. (2.5) can be integrated ($f=0.78$ for a vacancy mechanism) to give $k_p = 5.1 D^*(\mathrm{Co})$, where the diffusion coefficient is that at

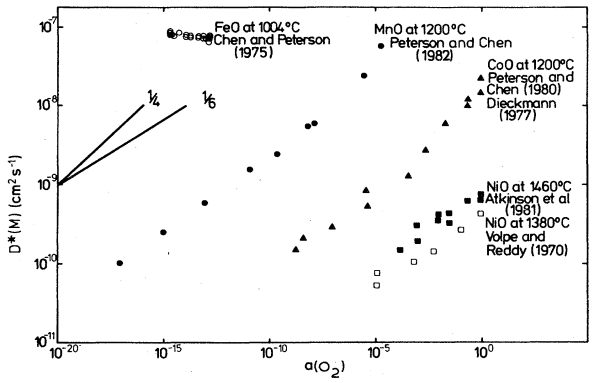

FIG. 9. Tracer self-diffusion coefficient, for lattice diffusion of metal ions in transition-metal oxides having the rocksalt structure, as a function of oxygen activity at selected temperatures. The solid lines show the slopes expected when either singly or doubly charged cation vacancies predominate in the oxide.

the activity of the oxide/gas interface. The theoretical rate constant obtained in this way for the oxidation of Co to CoO in air is compared in Fig. 10 with the most recent rate constants reported by Mrowec and Przybylski (1977). (Note that the growth rate is very rapid. Even at the lowest temperature the film grows to $\sim 30\ \mu$m in the first hour of oxidation.) The agreement is excellent at high temperatures (deviation less than 5%), and at the lowest temperatures the observed values are approximately 20% lower than the calculated ones. Gesmundo and Viani (1981) have used the approach based on point defects (Sec. II.A.2) to calculate k_p at 1000 °C, and their value is also shown in Fig. 10. It is lower than the other calculated value because it assumes a contribution to transport from uncharged cobalt vacancies. The observed value is about 10% greater than this calculated one. (Gesmundo and Viani concluded that the measured value was about 40% greater than their calculated one. This larger discrepancy appears to originate in their misquoting the results of Mrowec and Przybylski.)

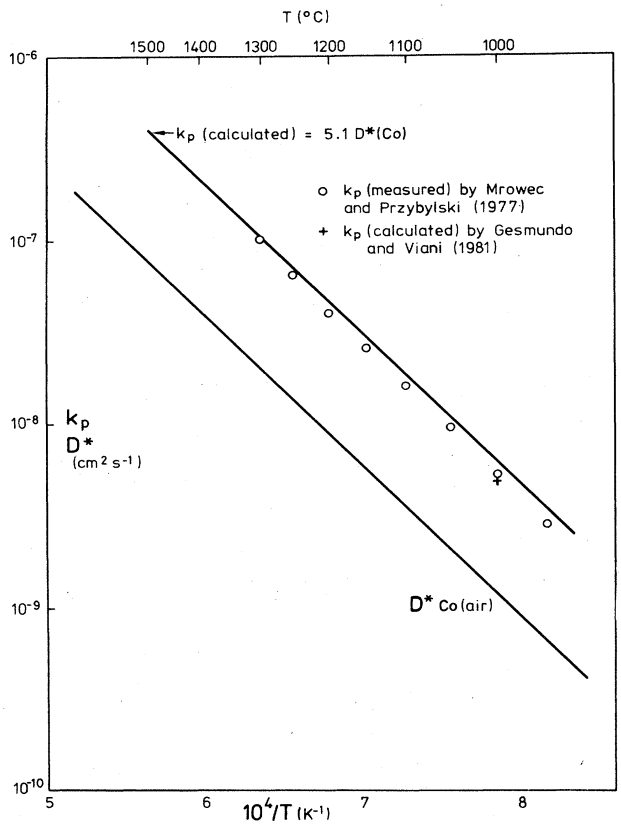

FIG. 10. Parabolic rate constant measured for the growth of thick CoO films on Co in air [$a(O_2)=0.21$] compared with that calculated using Wagner's theory and the tracer diffusion coefficient for Co in CoO, or the concentration and mobility of Co vacancies in CoO (Gesmundo and Viani, 1981).

The dependence of k_p on $a(O_2)$ measured by Mrowec and Przybylski is in agreement with the tracer diffusion studies to within experimental error. As the temperature is lowered the oxygen pressure dependence of k_p changes slightly from $a(O_2)^{1/4}$ at 1300 °C to $a(O_2)^{1/3.3}$ at 950 °C. This is consistent with a contribution from uncharged cobalt vacancies at the lower temperatures.

We can therefore conclude that the formation of CoO on Co at temperatures between 950 °C and 1300 °C establishes the Wagner theory as a good quantitative description of thick film growth. Those uncertainties which remain ($\sim 10\%$) are related to the precision of the experiments and to the finer details of the defect structure of CoO.

B. Growth of NiO

The crystal structure and defect properties of NiO are very similar to those of CoO, the main difference being that the defect concentrations are lower in NiO [$\sim 7\times 10^{-5}$ mole fraction of 1000 °C and $a(O_2)=1$, Atkinson, Hughes, and Hammou, 1981] than in CoO ($\sim 6\times 10^{-3}$ mole fraction). The diffusion of Ni in the NiO lattice is now reasonably well understood (e.g., Fig. 9) and has been shown to be unaffected by impurities (i.e., intrinsic) at temperatures as low as 500 °C [and $a(O_2)=1$] in crystals of a purity comparable to that obtainable in Ni (Atkinson and Taylor, 1979). We are thus in a position to make a comparison between Wagner's theory and experiment over a much wider range of temperature and growth rates than was possible for CoO.

1. Growth of thick NiO films at $T > 500$ °C

In the case of Ni oxidation, integration of Eq. (2.5) gives $k_p \approx 6.4 D^*(\mathrm{Ni})$, where the diffusion coefficient is again that at the oxygen activity of the oxide/gas interface. This is shown plotted in Fig. 11 in comparison with the measured values. The comparison is not so straightforward as it was for CoO growth, since the reported values of k_p for NiO show much greater scatter. This scatter has been shown to depend on metal purity, surface condition (Caplan *et al.*, 1972), and crystal orientation

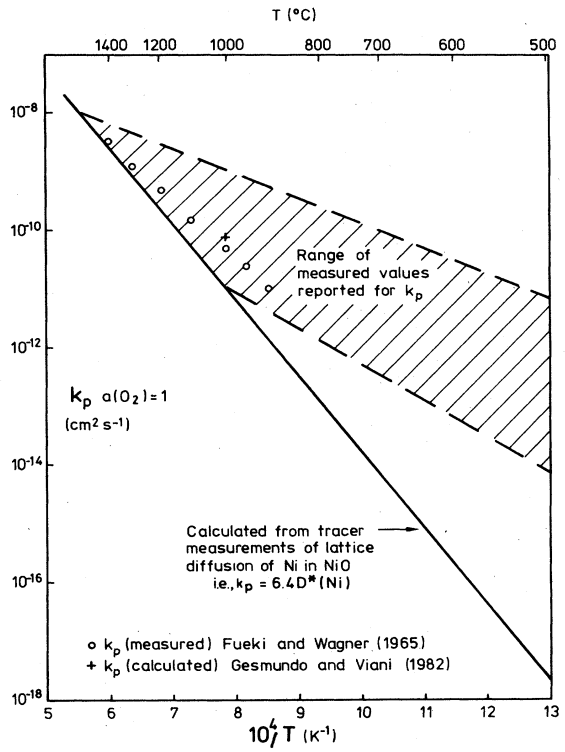

FIG. 11. Parabolic rate constant measured for the growth of NiO on Ni in oxygen [$a(O_2)=1$] compared with that calculated using Wagner's theory and the tracer diffusion of Ni in the NiO lattice, or the concentration and mobility of cation vacancies in NiO (Gesmundo and Viani, 1982).

(Khoi *et al.*, 1975). Furthermore, at the lower temperatures the kinetics are not parabolic, the exponent of t in $X \propto t^n$ being less than 0.5. Nevertheless, it can be clearly seen from Fig. 11 that the lower the temperature the greater is the measured "parabolic" rate constant compared with that predicted from Wagner's theory until, at 500 °C, it is 3—7 orders of magnitude greater.

At the highest temperatures (greater than 1200 °C) the agreement between measured and predicted values of k_p is reasonably good, as illustrated by the data of Fueki and Wagner (1965) in Fig. 11. They also found $k_p \propto a(O_2)^{1/n}$ with $3.5 < n < 6$. This is reasonably consistent with the diffusion measurements, although they observed significant and unexplained departure from the expected behavior for $a(O_2) \sim 1$. With the use of the same point defect approach as described for CoO, Gesmundo and Viani (1982) have predicted k_p at 1000 °C for NiO. This is also plotted on Fig. 11 and can be seen to be approximately seven times greater than that predicted from the tracer diffusion measurements. The reason for this difference is the uncertainty which exists concerning the concentrations and diffusivities of point defects in NiO (Atkinson, Hughes, and Hammou, 1981).

Several suggestions have been advanced to account for the observed k_p's being greater than predicted at the lower temperatures and for the scatter in the measurements. Berry and Paidassi (1966) first proposed that the high values of k_p were caused by impurities doping the oxide. While this may account for some of the variability, low-temperature diffusion measurements in oxide single crystals of a purity similar to that of the purest of the oxide films demonstrates that this is not the fundamental reason for the discrepancy. Young, Cathcart, and Gwathmey (1956) and later Perrow, Smeltzer, and Embury (1968) suggested that fast diffusion along oxide gain boundaries is responsible for the fast oxidation rates and that the variability in k_p reflects the variability in the type and density of the grain boundaries (Khoi, Smeltzer, and Embury, 1975). Rhines and Wolf (1970) proposed a radically different "swelling" mechanism for NiO film formation, in which the new oxide is formed at oxide grain boundaries by lattice diffusion of Ni and grain boundary diffusion of O. This proposition was mainly to account for the stresses which they inferred in growing NiO films and was subsequently developed to analyze oxide grain growth during Ni oxidation (Rhines and Connell, 1977; Rhines *et al.*, 1979).

In order to determine how large a contribution rapid diffusion along dislocations and grain boundaries could make to the growth rate, Atkinson and Taylor (1979,1981) studied the diffusion of Ni along such paths in NiO and the results are summarized in Fig. 12. In the

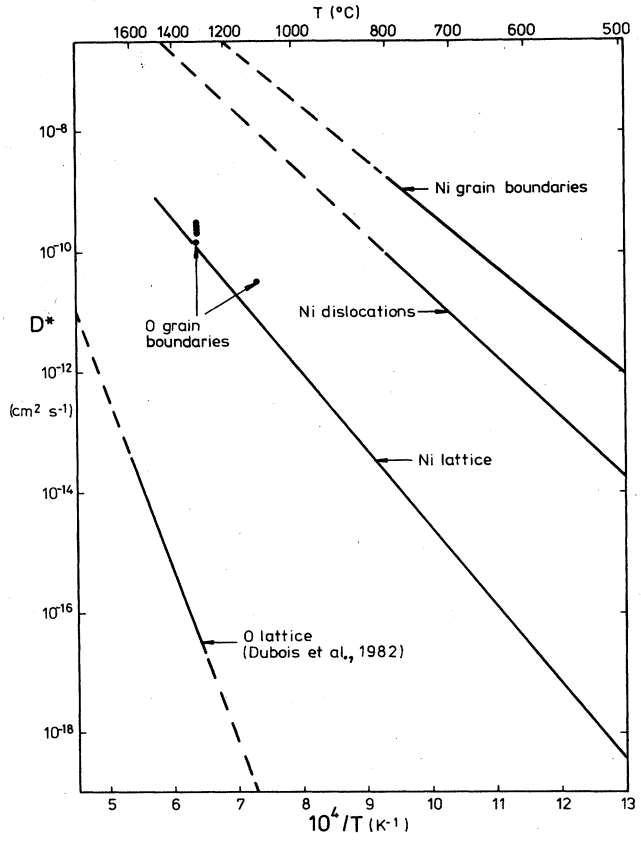

FIG. 12. Tracer diffusion coefficients measured as a function of temperature for Ni [at $a(O_2)=1$] and O [at $a(O_2)=0.2$] diffusion in the lattice and along dislocations and grain boundaries in NiO. Data for Ni diffusion are from Atkinson and Taylor (1979,1981).

case of grain boundaries, the experiments actually measure the product of the boundary diffusion coefficient (D') and the effective width of the boundary (δ), which was estimated to be ~ 1 nm in separate experiments. It can be seen from Fig. 12 that diffusion along dislocations is faster than in the lattice and that diffusion along grain boundaries is faster than along dislocations. The activation energies for lattice, dislocation, and grain boundary diffusion are 2.56, 2.00, and 1.78 eV per ion, respectively, and the similar dependence of all three diffusion coefficients on $a(O_2)$ suggests a vacancy mechanism in all cases. These data have been used (Atkinson *et al.*, 1982) to predict k_p when grain boundary diffusion is included, in which case

$$k_p = 6.4 \left[D^* + \frac{2(D'\delta)^*}{g} \right], \tag{3.1}$$

where the diffusion parameters are for Ni at the $a(O_2)$ of the oxide/gas interface. g is the grain size in the oxide film and was measured by transmission electron microscopy in the films for which the kinetic data were obtained. Figure 13 shows k_p calculated in this way compared with the measured value for temperatures between 500 °C and 800 °C and films ranging from 0.28 to 27.2 μm in thickness (grain sizes 0.15 to 1.4 μm). The agreement is excellent and proves that film growth is taking place by grain boundary diffusion in this temperature range. Also shown for comparison in Fig. 13 is the much lower k_p predicted from lattice diffusion. Furthermore, the departure from strict parabolic kinetics is seen to be a result of grain growth which reduces the density of fast-diffusion paths. The same mechanism also accounts for the growth rates and kinetics observed by Rhines and Connell (1977) in the temperature range 800 °C—1000 °C for films up to 32 μm in thickness and grain size up to 4.5 μm. In the temperature range 500 °C—1000 °C the apparent activation energy of k_p is ~ 1.5 eV. This is less than the 1.78 eV for grain boundary diffusion itself, because the grain size in the oxide is smaller the lower the temperature.

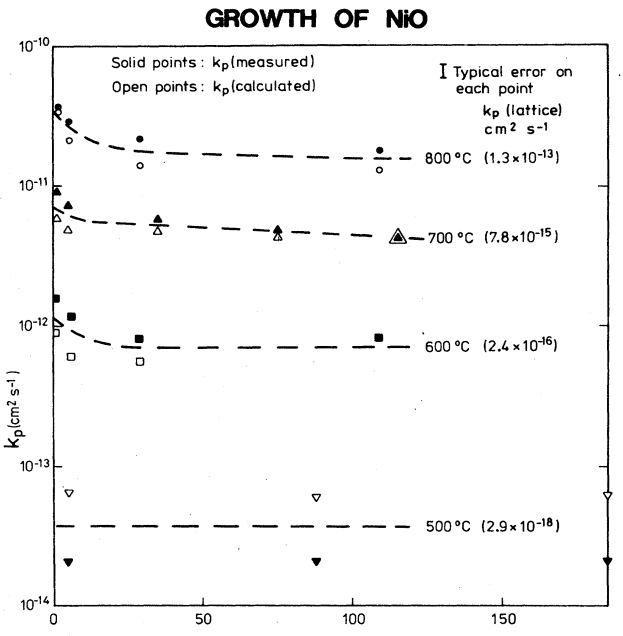

FIG. 13. Parabolic rate constant as a function of time for the growth of NiO on Ni at temperatures in the range 500 °C—800 °C and $a(O_2)=1$. The points plotted with open symbols have been calculated from tracer diffusion data, and measurements of oxide grain size, using Wagner's theory modified to include grain boundary diffusion in the oxide. The much lower values expected from lattice diffusion alone are shown in parentheses. (Atkinson, Taylor, and Hughes, 1982.)

Recent measurements of the diffusion of O in NiO grain boundaries (Atkinson *et al.*, 1985) are also shown in Fig. 12 and are seen to be of the same order as the lattice diffusion coefficient of Ni. Although these data are for relatively high temperatures, it is reasonable to conclude that the solid-state diffusion of O makes no significant contribution to NiO film growth. The movement of both metal and oxygen during film growth has been studied using ^{63}Ni and ^{18}O tracers in experiments of the type described in Sec. II.D (Atkinson *et al.*, 1979). The results of these experiments are entirely consistent with the above mechanism in which outward diffusion of Ni along NiO grain boundaries is the dominant transport process at temperatures below 1000 °C (except under conditions where two-layered, or duplex, films are formed, in which case there is significant inward transport of oxygen; see Sec. V.A).

We have thus seen that the Wagner theory when modified to include grain boundary diffusion can account for the oxidation of Ni at temperatures above 500 °C and for films greater than ~ 0.3 μm in thickness. This is gratifying, since all such films are thicker than the Debye length (Fig. 3), which marks the lower bound of applicability of Wagner's theory. We will now consider the growth of thinner films at temperatures below 500 °C.

2. Growth of thin NiO films at $T < 500$ °C

The very early stages of the oxidation of single-crystal Ni surfaces (i.e., the chemisorption and nucleation stages) at very low pressures (10^{-11}—10^{-9} atm) and temperatures in the range 65 °C—300 °C have been studied using Auger electron spectroscopy by Liu, Armitage, and Woodruff (1982). They found that the rate of oxygen uptake (corresponding to only two or three monolayers total thickness) of the major crystal faces is in the order {111} > {110} > {100}, which they explained in terms of the denser packing of adsorbed oxygen which is possible on the {111} face and which in turn is more favorable for nucleation of the bulk oxide from the adsorbed layer. Similar studies of the {100}, {110} (Mitchell, Sewell, and Cohen, 1976, and 1977), {111}, and {211} (Mitchell and Graham, 1982) faces of Ni have used reflection high-energy electron diffraction (RHEED) in combination with surface analysis for films up to ~ 2 nm in thickness. An example of their kinetic data, which they divide into three stages, is shown in Fig. 14. The first stage is chemisorp-

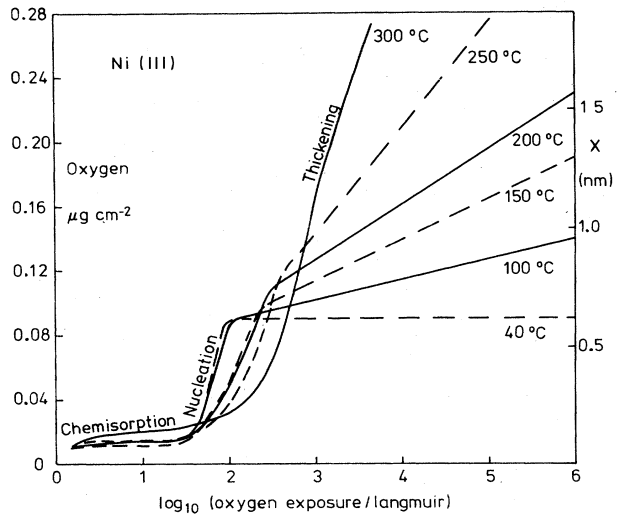

FIG. 14. Uptake of oxygen on the (111) crystal face of Ni as a function of oxygen exposure at low temperatures and low oxygen pressures (10^{-12}–10^{-10} atm). 1 langmuir is an exposure of 10^{-6} Torr s, and a "monolayer" of NiO parallel to the (111) NiO plane has a thickness of 0.241 nm (0.0351 μg O cm^{-2}). The regimes interpreted as chemisorption, oxide nucleation, and film thickening are indicated (after Mitchell and Graham, 1982).

tion, the second is the nucleation and lateral growth of NiO islands of approximately 0.7 nm thickness, and the final stage (which is absent at 40 °C) is a logarithmic thickening of the film. The diffraction data show that the oxide is crystalline and initially epitaxially related to the metal with {100} oxide planes parallel to {100} and {110} metal surfaces and {111} oxide planes on {111} and {211} metal surfaces. The films were polycrystalline or single crystal depending on the oxidation conditions. In the film-thickening stage the kinetics could be described by a direct logarithmic growth law with a low activation energy of ~0.3 eV. In all stages of the reaction the oxide thickness was a function of the oxygen exposure, i.e., $X=f(pt)$. This means that at a given oxide thickness the growth rate is proportional to the oxygen pressure for pressures in the range 10^{-11}–10^{-7} atm.

Graham and Cohen (1972) studied the oxidation of polycrystalline Ni at higher pressures (7×10^{-6} to 8×10^{-4} atm) and to higher temperatures (23 °C–450 °C). The kinetics of the first two stages (chemisorption followed by nucleation and lateral growth) were not resolved in these earlier experiments, probably because of their greater rapidity at the higher pressures. At temperatures below 300 °C logarithmic kinetics were observed and the films tended towards a limiting thickness (different for different temperatures). For temperatures above 300 °C and film thicknesses greater than 3 nm, a fourth stage was observed (and followed in films up to 1 μm in thickness) in which the kinetics were parabolic. The parabolic rate constant was found to be approximately proportional to $a(O_2)^{1/6}$ and had an activation energy of 1.8 eV.

This parabolic behavior is so similar to that observed at 500 °C and above that it suggests that the mechanism remains the same down to 300 °C and films only 3 nm in thickness. The activation energy for k_p is also in agreement with that measured for grain boundary diffusion (1.78 eV), although this may be somewhat fortuitous, since the variation of oxide grain size with temperature would lead us to expect a slightly lower activation energy for oxidation. Referring to Fig. 3, we see that these films are not in a region in which the assumption of electrical neutrality is expected to be valid, since at 300 °C the Debye length is estimated to be ~1 μm in stoichiometric NiO. For a growing oxide film the effective Debye length may be considerably less than this, either because of small concentrations of charged impurities (~1 in 10^6), or because the intrinsic defect concentrations are much larger in the dominant diffusion paths (such as grain boundaries) than in the bulk. Ritchie, Scott, and Fensham (1970) observed that when an electric field was applied to a growing NiO film at temperatures above 350 °C, the rate increased when the oxide/gas interface was negatively biased. This merely indicates that film growth is occurring by the movement of ions and does not distinguish between control by ionic or electronic transport (see Sec. II.C.1).

However, for temperatures below ~300 °C, where the oxidation kinetics are logarithmic the mechanism is not so clear. We will analyze the experiments in terms of the Cabrera and Mott mechanism, beginning with the limiting oxide thickness (X_L) as a function of temperature and the transition temperature above which parabolic kinetics are observed. The criterion for this latter transition is when $W/kT=40$ (Sec. II.B). Using the same approximations suggested in Sec. II.C.2, we deduce that for cation transport along oxide grain boundaries $W=1.78$ eV and hence the transition temperature is ~250 °C. This is in reasonable agreement with the observation of ~300 °C. For temperatures below the transition temperature we can use Eq. (2.33) to calculate the limiting oxide thickness (based on the Cabrera and Mott criterion of when the growth rate is less than 10^{-15} ms^{-1}) as a function of temperature. The solid lines in Fig. 15 are calculated in this way with values of W corresponding to lattice diffusion (2.56 eV) and grain boundary diffusion (1.78 eV). In order to calculate X_1 we have approximated $\Delta\varphi$ by $-\Delta G^\circ(\text{NiO})/2e$. Experimental values of the limiting thickness are also plotted in Fig. 15, and it can be seen that a value of ~2 eV for W will explain the observations. However, such a value of W is not compatible with the low activation energy observed for the logarithmic rate constant (0.3 eV).

This may possibly be accounted for by a reanalysis of the kinetic data in terms of the Cabrera and Mott model rather than the direct logarithmic kinetics which were used in the original papers. Fehlner (1984) has recently analyzed the data of Graham and Cohen (1972) in terms of the Cabrera and Mott theory using the method suggested by Ghez (1973). Fehlner concludes that the data can be just as well described by Cabrera and Mott kinetics as by direct logarithmic kinetics. Furthermore, the activa-

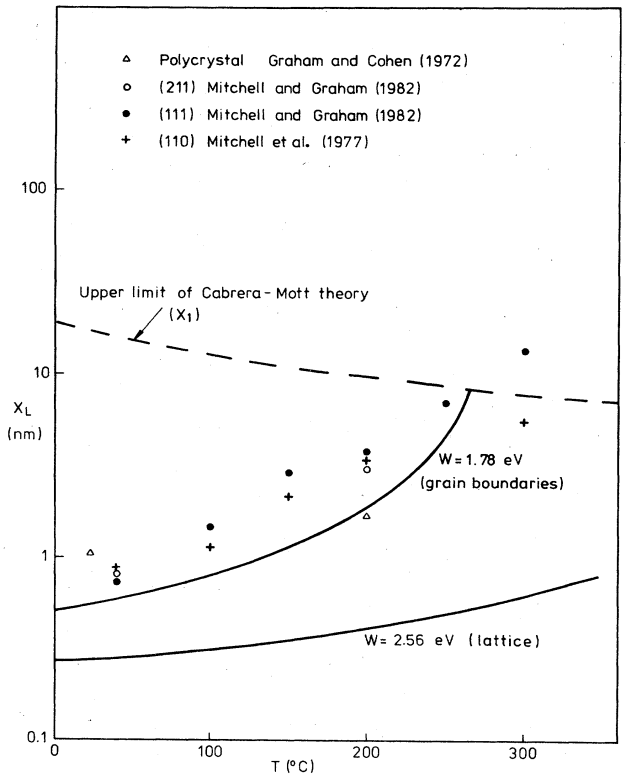

FIG. 15. Limiting oxide film thickness in the oxidation of Ni at low temperature plotted as a function of temperature. The limiting thickness is that beyond which the film growth rate is negligibly slow ($<10^{-15}$ ms^{-1}). The solid lines are calculated from the theory of Cabrera and Mott with values of W corresponding to migration of Ni ions either along grain boundaries or through the lattice.

tion energy for the rate constant [W in Eq. (2.26)] is 1.6 eV and the built-in voltage $|\Delta\varphi|$ is $\simeq$2.4 V. When the single-crystal data (Mitchell *et al.*, 1976,1977,1982) are reanalyzed in the same way, W is found to be about 2 eV and $|\Delta\varphi|$ in the range 1.5—2.5 V. These values for W are consistent with that required to explain the limiting thickness in the logarithmic region and with the activation energy of the low-temperature parabolic rate constant (which was argued earlier to be controlled by grain boundary diffusion). The observed linear dependence of growth rate on oxygen pressure at low pressures in the logarithmic region probably indicates that at these low pressures the sites for defect injection into the oxide are those next to a diatomic species of adsorbed oxygen (e.g., O_2^-). The only experimental observation that cannot be rationalized on this basis is the reversal of the effect of an applied electric field at temperatures below 350 °C (Ritchie, Scott, and Fensham, 1970).

C. Growth of iron oxides

The oxidation of iron introduces an additional complication because of the different iron oxides which can form, namely, wüstite ($Fe_{1-x}O$), magnetite (Fe_3O_4), hematite (Fe_2O_3), and the metastable oxide γ-Fe_2O_3. The oxidation of Fe in air in temperatures above 570 °C results in a scale with three layers, an inner wüstite layer, a thinner middle layer of magnetite, and an even thinner outer layer of hematite. Yurek *et al.* (1974) have shown how to relate the observed parabolic rate constant for the growth of a phase in such a multilayered scale to the notional parabolic rate constant which would be measured if the single phase were able to grow on the metal over the same range of oxygen activities, i.e., k_p as given by Eq. (2.5) but with $a(O_2)_I$ and $a(O_2)_{II}$ being the limits of oxygen activity across the phase when growing in the multilayer scale. Such an analysis, in common with the Wagner theory, assumes that all interfacial reactions are sufficiently rapid not to be rate limiting. Garnaud and Rapp (1977) have applied this theory successfully to the oxidation of Fe.

The growth of wüstite on Fe is so rapid that low-alloy steels cannot be contemplated for use at temperatures above 570 °C (the lowest temperature at which wüstite is stable). But even though wüstite is of no value as a protective oxide, its growth is of interest, because it has such a high concentration of point defects that complex defect aggregates are formed. In common with other transition-metal oxides having the rocksalt structure (NiO, CoO), wüstite is cation deficient, but the deficiency can be as much as 16% ($Fe_{0.84}O$). Tracer diffusion studies by Chen and Peterson (1975) show that diffusion of Fe takes place by "free" vacancies which are in equilibrium with other relatively immobile vacancies bound in clusters. As a result, the tracer diffusion coefficient does not necessarily increase as the departure from stoichiometry increases (as it does in NiO and CoO), but, in the range 1000 °C—1200 °C, is approximately independent of composition (see Fig. 9). Since Wagner's theory is phenomenological, its application is independent of the complex point defect interactions, and Garnaud and Rapp (1977) have applied it to wüstite formation at 1100 °C and found that the observed and calculated parabolic rate constants agree to within 8%.

The growth of magnetite is of much greater technological importance, since magnetite films are relied upon to protect low-alloy steels when used at temperatures below 570 °C. The tracer diffusion of Fe in magnetite has been studied at high temperatures (900 °C—1400 °C) by Dieckmann and Schmalzried (1977) and Peterson *et al.* (1980) and shown to occur by a vacancy mechanism at high oxygen activity and by an interstitial mechanism at low oxygen activity. Atkinson and Taylor (1983) have shown that the same lattice diffusion mechanisms are valid at the much lower temperature of 500 °C, i.e., in the temperature region of technological interest. These tracer diffusion data are summarized in Fig. 16. The maximum value of the parabolic rate constant for magnetite formation [i.e., when $a(O_2)_I$ and $a(O_2)_{II}$ are the stability limits of magnetite] predicted from the diffusion data using Wagner's theory is plotted in Fig. 17 and compared with measured values taken from the literature. At high tem-

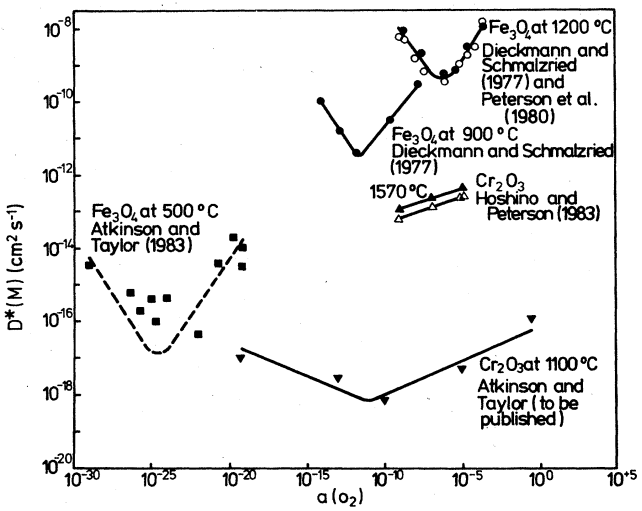

FIG. 16. Tracer self-diffusion coefficient for lattice diffusion of cations in Fe_3O_4 and Cr_2O_3 as a function of oxygen activity. The lines have the predicted slopes for diffusion by vacancies at the higher oxygen activities and interstitials at the lower. The two sets of data for Cr_2O_3 at 1570 °C are for diffusion parallel and perpendicular to the hexagonal axis.

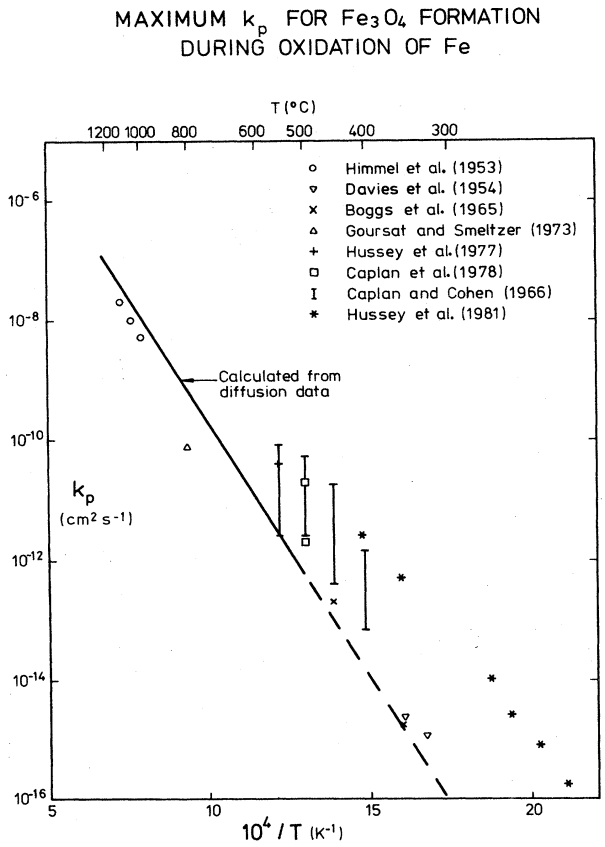

FIG. 17. Maximum parabolic rate constant (see text) for Fe_3O_4 film growth compared with that calculated using Wagner's theory and data for tracer diffusion of Fe in the Fe_3O_4 lattice.

peratures (>700 °C) the agreement is good and also consistent with the rate of formation of magnetite by the solid-state reaction of wüstite and hematite (Dieckmann, 1984). Wagner's theory would be expected to be valid down to the very thin film region (<20 nm), since the electronic conductivity of bulk Fe_3O_4 is so large, due to electron hopping between Fe^{2+} and Fe^{3+} ions, that the Debye length is always extremely small. At temperatures below 700 °C there is a tendency for the observed values of k_p to be more widely scattered and greater than the predicted values (Fig. 17). Although this effect is not so marked as in the growth of NiO (Fig. 11), the behavior is sufficiently similar to strongly suggest that at these lower temperatures the growth of Fe_3O_4 is controlled by the outward diffusion of Fe along oxide grain boundaries. This mechanism is supported by the observed movement of ^{55}Fe and ^{18}O tracers during the growth of Fe_3O_4 films (Atkinson and Taylor, 1982).

The growth of Fe_2O_3 during the oxidation of Fe has not been much studied, because its growth is much slower than the other iron oxides and because it appears as only a thin film on the outer surface of the much thicker layers of wüstite and magnetite. The published data for tracer diffusion in bulk Fe_2O_3 [see Kofstad (1972)] indicate that Fe and O have comparable diffusion coefficients, and it is not clear which species is likely to be rate controlling during film growth. Francis and Lees (1976) used ^{18}O tracers to study the growth of Fe_2O_3 during the oxidation of Fe at the relatively low temperature of 550 °C, since conflicting conclusions had been drawn from earlier marker studies. They concluded that the Fe_2O_3 was growing both by the outward solid-state transport of Fe and the inward transport of oxygen, possibly along cracks. The activation energy for Fe_2O_3 formation (1.75—2.30 eV) is considerably less than the reported activation energies for either Fe (4.0—4.9 eV) or O (3.4—6.3 eV) lattice diffusion, which perhaps suggests that transport occurs by faster short-circuit paths of lower activation energy (Channing and Graham, 1972; Goursat and Smeltzer, 1973). However, the current level of understanding of diffusion processes in Fe_2O_3 and the mechanism of Fe_2O_3 film growth is sufficiently poor to warrant further clarification.

D. Growth of Cr_2O_3

The sesquioxide Cr_2O_3, which is isostructural with Fe_2O_3, is the only solid oxide that is formed by the thermal oxidation of Cr. Cr_2O_3 is an extremely important oxide technologically, since it is the major constituent of the protective films which grow on stainless steels and many other heat-resistant alloys. Consequently, the literature contains many studies of the formation of Cr_2O_3 films.

1. Growth of thick Cr_2O_3 films

The formation of Cr_2O_3 by the oxidation of Cr at high temperatures has been reviewed recently in a series of arti-

cles by Lillerud and Kofstad (Lillerud and Kofstad, 1980; Kofstad and Lillerud, 1980,1982; Lillerud and Kofstad, 1982a,1982b) and by Hindam and Whittle (1983). The interpretation of oxidation kinetics in this system is greatly complicated by various departures from ideal behavior such as the volatilization of CrO_3 (particularly at temperatures above 1000 °C and oxygen pressures above 10^{-5} atm), loss of contact between metal and film, and cracking and blistering of the film. Nevertheless, many workers have been able to extract parabolic rate constants for the reaction and these have been summarized by Lillerud and Kofstad (1980) and are shown in Fig. 18. The results, not unexpectedly in view of the complications, show wide scatter and, in common with NiO and Fe_3O_4, a sensitivity to the way in which the metal surface was prepared. The lowest rate constants (in the high-temperature region) were measured by Caplan and Sproule (1975) on certain parts of a chemically etched Cr specimen. The pressure dependence of k_p is difficult to determine, since different kinetics may be observed in different ranges of $a(O_2)$ [e.g., Lillerud and Kofstad (1980)]. Kassner *et al.* (1966) report k_p's increasing with $a(O_2)$ at low values of $a(O_2)$ and for temperatures in the range 700 °C—1000 °C. On the other hand, Hindam and Whittle (1983) found k_p to be almost independent of $a(O_2)$ in the range 10^{-8} to 10^{-14} at 1000 °C.

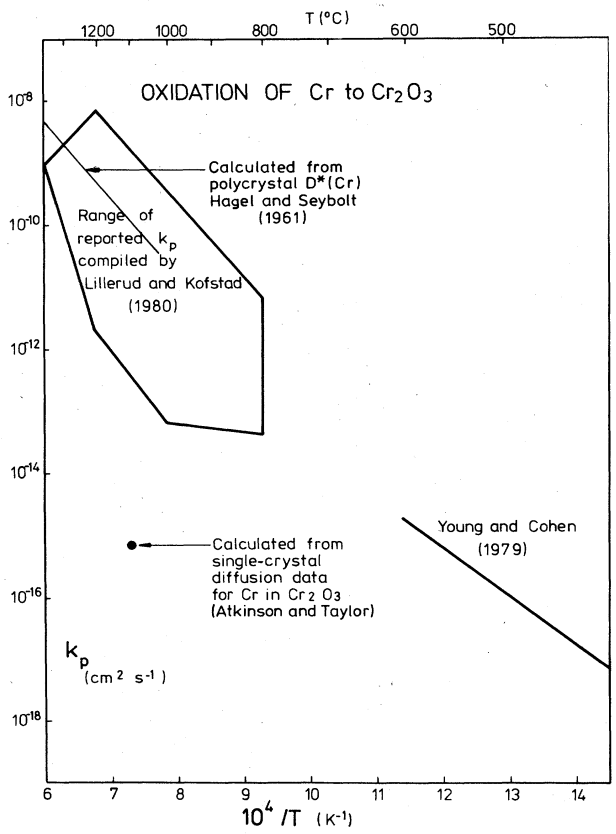

FIG. 18. Parabolic rate constant for growth of Cr_2O_3 films as a function of temperature. The parabolic rate constants have also been estimated using Wagner's theory and two widely differing sets of data for diffusion of Cr in the Cr_2O_3 lattice.

The current view of the point defect properties of Cr_2O_3 has been summarized by Kröger (1983). The oxide can be either a *p*-type or an *n*-type semiconductor, depending on doping and $a(O_2)$, but the point defects responsible are still a subject of controversy. The most commonly held view is that Cr_2O_3 is a *p*-type conductor at high $a(O_2)$ and low temperatures, but is "intrinsic" (i.e., with band-to-band excitations) at temperatures above ~1200 °C. Diffusion of Cr in Cr_2O_3 has been studied by several workers, but the results are not in agreement. The most recent data from Hoshino and Peterson (1983) and Atkinson and Taylor (1985) for $D^*(Cr)$ are shown in Fig. 16. These measurements are 4—7 orders of magnitude lower than the previously published data. The reason for the high earlier values appears to be that they were dominated by dislocation and grain boundary effects. At high $a(O_2)$ the lines on Fig. 16 correspond to $D^*(Cr) \propto a(O_2)^{3/16}$, which is the dependence expected from the reaction

$$\tfrac{3}{2}O_2 \rightarrow 3O_O^x + 2V_{Cr}''' + 6\dot{h} \tag{3.2}$$

and the electroneutrality condition $3[V_{Cr}'''] = [\dot{h}]$. This seems reasonable at 1100 °C, but at ~1500 °C Cr_2O_3 is believed to be an "intrinsic" electronic conductor with the electroneutrality condition $[\dot{h}] = [e']$. Therefore $D^*(Cr) \propto a(O_2)^{3/4}$ would be expected at temperatures above ~1200 °C, and this is not observed experimentally. At low $a(O_2)$ at 1100 °C the diffusion data suggest diffusion by Cr interstitials formed by the reaction

$$Cr_2O_3 \rightarrow \tfrac{3}{2}O_2 + 2Cr_i^{\cdots} + 6e' , \tag{3.3}$$

from which $D^*(Cr) \propto a(O_2)^{-3/16}$ is expected.

Kofstad and Lillerud (1980) used the earlier data for $D^*(Cr)$ to calculate k_p from Wagner's theory and assumed reaction (3.3) was dominant. The predicted values fall within the range of the measured values, as shown in Fig. 18. However, in light of the more recent diffusion experiments, this agreement appears to be fortuitous. The parabolic rate constant predicted from the recent diffusion data is also shown in Fig. 18 and is approximately 5 orders of magnitude lower than the earlier predictions. The most likely explanation is that those same fast-diffusion paths (grain boundaries and dislocations) which perturbed the earlier diffusion experiments are the dominant transport paths in film growth. Indeed, the diffusion profiles in single crystals observed by Atkinson and Taylor (1985) show a large contribution from diffusion along low-angle grain boundaries, but this in itself is not able to account for the rate of growth of Cr_2O_3. Presumably, by analogy with NiO, diffusion along high-angle boundaries is faster.

2. Growth of thin Cr_2O_3 films

Hope and Ritchie (1976) and Young and Cohen (1977a,1977b) have studied the growth of thin films on Cr at temperatures in the range 225 °C—600 °C. The films

were fine-grained polycrystalline Cr_2O_3. The experiments show only logarithmic-type kinetics for temperatures below ~400 °C and logarithmic followed by subsequent parabolic kinetics at higher temperatures. This is similar to the situation found for NiO growth, and the transition temperature of 400 °C, when interpreted according to the Cabrera and Mott model, corresponds to $W \sim 2.3$ eV.

Hope and Ritchie carried out electrical marker experiments in the temperature range 225 °C—425 °C (i.e., spanning the transition temperature) and deduced that only Cr was mobile in the oxide film. This is consistent with the recent $^{16}O_2/^{18}O_2$ sequential oxidation experiments of Mitchell *et al.* (1983) in a thin film (47 nm) at 700 °C. Hope and Ritchie also studied the effect of an applied field above and below the transition temperature. In both regions the rate increased when the oxide/gas interface was biased negatively, which is consistent with rate control by either ionic or electronic transport. (N.B. This is different from the growth of NiO, which shows the opposite field effect at temperatures below 350 °C.) Therefore, the growth of Cr_2O_3 is limited by the transport of Cr ions over the entire temperature range.

Young and Cohen (1977a) have analyzed the growth kinetics in the logarithmic region in terms of the Cabrera and Mott mechanism. The value of W from the kinetics is 1.9 eV, which is fairly consistent with W deduced from the transition temperature (2.3 eV). Furthermore, the measured rates of growth are in reasonable quantitative agreement (to within an order of magnitude) with those predicted by Eq. (2.31). They also studied the effect of $a(O_2)$ on the growth rate (Young and Cohen, 1977b). They found that increasing $a(O_2)$ always increased the growth rate, and that the dependence was approximately $a(O_2)^{0.1}$, which is consistent with the low sensitivity to $a(O_2)$ expected from the Cabrera and Mott theory. We may therefore conclude that this theory explains growth in the logarithmic region very well.

The rate constants from the parabolic region are plotted in Fig. 18 for comparison with the high-temperature data. Despite the large uncertainties it does not seem unreasonable to attribute a single process to the whole temperature range. The activation energy of Young and Cohen's parabolic rate constant is 1.6 eV, which is approximately consistent with W from the logarithmic regime. Therefore, behavior over the entire temperature range can be attributed to control by the transport of Cr along Cr_2O_3 grain boundaries. The only problem with this generalization is that Young and Cohen (1977b) observed k_p in the low-temperature region to decrease as $a(O_2)$ increased, a finding which cannot be explained in terms of Wagner's theory. This anomalous behavior was explained by Young and Cohen in terms of the nonuniform (nodular) morphology of the film in the low-temperature parabolic region. They postulated that the thin parts of the film are not contributing to total growth, but are controlling the concentration of injected defects, as in the logarithmic region. The low-temperature parabolic region (which extends to films as thin as 6 nm) is therefore not a simple extension of the thick film (Wagner) parabolic region. This contrasts with the growth of NiO, for which the same parabolic growth appears to be occurring for all films thicker than 3 nm when T is above the logarithmic-parabolic transition temperature.

E. Growth of Al_2O_3 films

Since Al metal melts at 660 °C, the growth of Al_2O_3 on solid substrates at high temperatures can only be studied using alloys of Al with more refractory metals. However, it is in this context that the growth process is of great interest, because Al_2O_3 is the most protective oxide against high-temperature corrosion. At high temperatures (> 1000 °C) the oxide that forms is α-Al_2O_3, which is isostructural with Cr_2O_3 and α-Fe_2O_3. At lower temperatures the oxide film usually comprises some of the metastable forms of Al_2O_3, particularly γ-Al_2O_3.

The protection at high temperatures afforded by α-Al_2O_3 is obviously the result of this oxide having low concentrations and mobilities of ionic and electronic defects. However, it is for this same reason that the defect properties of the α-Al_2O_3 are poorly understood, despite the technological importance of the oxide not only as a protective film but also as an engineering ceramic. The current understanding of defects and transport in α-Al_2O_3 has been summarized by Kröger (1983). The concentrations of intrinsic point defects are so low in this material that it seems likely that all reported properties relating to point defects and transport have been dominated by solute ions, present either as unavoidable impurities or deliberate dopants. According to Kröger, ionic defects are always more numerous than electronic defects, but since the latter have the higher mobility, the ionic contribution to conductivity is not always dominant. Whether ionic or electronic conductivity dominates is dependent in a complicated manner on T, $a(O_2)$, and doping. For example, Yee and Kröger (1973) report an ion transport number of approximate unity in a variety of single crystals at high $a(O_2)$ in the temperature range 1000 °C—1400 °C. They also found $t_{ion} \ll 1$ in polycrystalline material under similar conditions. However, the impurity-dominated nature of this oxide makes it dangerous to extend such data to the oxide of a growing film.

Sheasby and Jory (1978) have attempted to measure the electrical properties of Al_2O_3 growing at 1100 °C on Pt alloyed with 22 wt. % Al. They found that the open-circuit voltage was positive with respect to the alloy, as expected in all cases from Sec. II.A. However, the open-circuit voltage was found to decrease with oxidation time from ~1 V to ~0.2 V over the first 300 h. From Eq. (2.8) the open-circuit voltage should have been 2.12 V if the oxide film were an ionic conductor. Thus the measured voltage at long times indicates that $t_{ion} \sim 0.1$, and the film is therefore predominantly an electronic conductor. This is consistent with the example of bulk polycrystalline material cited earlier. It will now be evident that a detailed application of Wagner's theory to Al_2O_3 growth is fruit-

less because of the uncertainties concerning the defect and transport properties of the oxide in the film itself. Nevertheless, we can make some rather crude estimates if we assume, as seems reasonable, that electronic conductivity is dominant in the growing film and that the Debye length is not as great as suggested by the electrical conductivity (several mm at 1000 °C, Fig. 3).

Hindam and Whittle (1983) have compiled values of the "parabolic rate constant" for the growth of Al_2O_3 and these are shown in Fig. 19. In common with the growth of NiO and Cr_2O_3, the growth of Al_2O_3 is not strictly parabolic, and the rate constants which are included are those appropriate to relatively long exposure times. It is surprising that, in view of the variability in the properties of Al_2O_3, the scatter of experimental results is relatively narrow. Also plotted in Fig. 19 are several determinations of lattice diffusion in Al_2O_3. Data for Fe and Cr have been included to support the only measurements of Al self-diffusion by Paladino and Kingery (1962). They used large-grained (130 μm) polycrystalline specimens, and therefore there may have been some enhancement of the apparent diffusion coefficient due to grain boundary diffusion. All the diffusion coefficients are for anneals in air [$a(O_2)=0.21$], except for Reed and Wuensch's (1980) ^{18}O measurements. The oxygen activity was not defined in these experiments, but was below 10^{-8}. Lloyd and Bowen (1981) were the only investigators to vary the oxygen activity. They made measurements of D^*(Fe) for $a(O_2)$ in the range 10^{-9}–0.21. They found a tendency for D^* to increase with $a(O_2)$, which they interpreted in terms of diffusion by vacancies in a defect structure controlled by Si impurities. They proposed that the dependence on $a(O_2)$ is the result of Si^{x}_{Al} changing to $Si^{\cdot}_{Al}$, i.e., Si^{3+} to Si^{4+}. Whatever the validity of the interpretation, the important point relevant to the growth of Al_2O_3 films is that cation diffusion in Al_2O_3 is probably a weak function of $a(O_2)$, changing at the most by an order of magnitude over the range investigated. This is supported by the electrical conductivity measurements (Kröger, 1983).

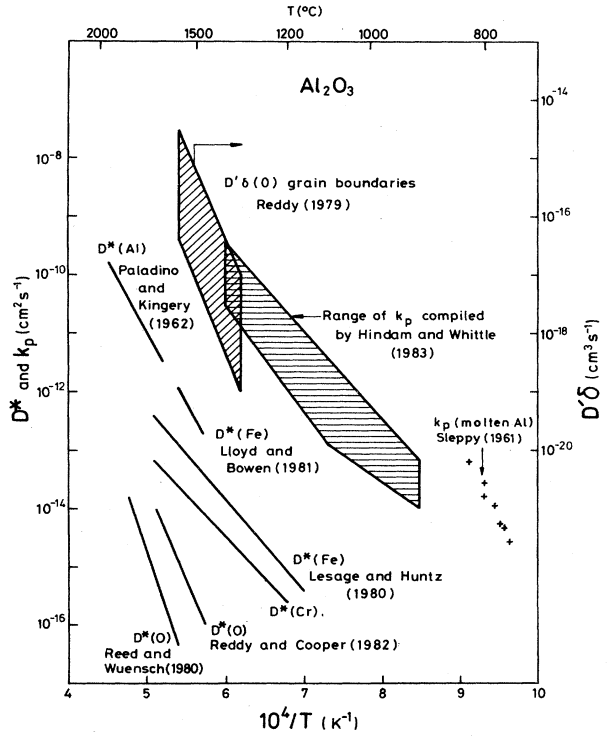

FIG. 19. Arrhenius plot comparing the parabolic rate constant for the growth of Al_2O_3 films and diffusion data in Al_2O_3. The scale for the grain-boundary diffusion parameter of oxygen is on the right and has been adjusted so that if $\delta=1$ nm the grain-boundary diffusion coefficient is given directly by the scale on the left.

Returning to Fig. 19, we therefore conclude that D^*(Al) is always greater than D^*(O) in the Al_2O_3 lattice and that D^*(Al) is too slow by at least 2 orders of magnitude to account for the lowest k_p measured at the highest temperature (1400 °C). It has generally been inferred from studies of scale morphology and the behavior of impurity markers that Al_2O_3 grows by the inward migration of oxygen. Reddy *et al.* (1982) have reported two-stage $^{16}O_2/^{18}O_2$ tracer experiments for the growth of Al_2O_3 on NiCrAl alloys at 1100 °C. Their results show that the ^{18}O tracer passes through the ^{16}O film with very little exchange. This not only confirms that inward oxygen transport is dominant, but also that the diffusion paths are short-circuit ones, such as fissures or grain boundaries. Reddy (1979) also measured $D'\delta$ for ^{18}O diffusion in grain boundaries in polycrystalline Al_2O_3. The results, which show wide scatter, are also summarized in Fig. 19. The relative scales of $D'\delta$ and D^* have been chosen such that if $\delta=1$ nm (as is known to be the case in NiO) the values of D' are read directly on the diffusion coefficient scale. If we compare $D'\delta$(O) with D^*(Al) we would expect grain boundary transport of oxygen to be equivalent to lattice transport of Al in a material with grain size ~ 1 μm at 1600 °C. It is therefore not possible to deduce from the existing tracer results in bulk specimens, whether oxygen grain boundary transport would be more effective for film growth than Al lattice transport. Measurements of both Al and O tracer diffusion in the same sample would ideally be required to answer this question. Similarly, Reddy's measured values of $D'\delta$(O) are not large enough to account for the lowest values of k_p by approximately 2 orders of magnitude when allowance is made for grain size. Nevertheless, grain boundary diffusion of oxygen is the most likely transport process controlling the growth of Al_2O_3 films at high temperatures.

The growth of Al_2O_3 films at relatively low temperatures has not been studied recently. The oxide film is amorphous at temperatures below 400 °C. Hunt and Ritchie (1970) measured the electrical properties of such films and concluded that electronic conductivity was dominant ($t_{ion}\sim 10^{-6}$) and that the films grew by the outward migration of Al interstitial ions (cf. O migration at high temperatures). The growth rate increased when the oxide/gas interface was biased negatively, again indicating transport by ions and electrons. The magnitude of the effect of the applied electric field was consistent with that

expected for growth according to the Cabrera and Mott mechanism.

Sleppy (1961) studied the growth of Al_2O_3 films on molten Al at temperatures in the range 660 °C—850 °C. He found logarithmic-type kinetics at temperatures below 700 °C and mainly parabolic at higher temperatures. The parabolic rate constants are plotted in Fig. 19 and are seen to be compatible with those measured on alloys despite the fact that the oxide growing on molten Al was deduced to be η-Al_2O_3 rather than α-Al_2O_3.

IV. OXIDATION OF SILICON

The rate of growth of SiO_2 films (which are always amorphous) is slow and they may be classed with those of Cr_2O_3 and Al_2O_3 as being among the most protective from the point of view of oxidation resistance. However, the thermal expansion coefficient of amorphous SiO_2 is very low (0.45×10^{-6} K^{-1}), and the expansion mismatch stresses which result from thermal cycling are usually sufficient to cause the film to detach from most alloy substrates. This has limited the usefulness of SiO_2 as a protective oxide on high-temperature alloys. Fortunately for semiconductor technology, the thermal expansion coefficient of Si (3×10^{-6} K^{-1}) is much lower than that of most metals ($\sim15\times10^{-6}$ K^{-1}), and adherent dielectric SiO_2 films may be grown on Si by thermal oxidation for device fabrication. It is therefore for such applications that the oxidation of Si to SiO_2 has received a great deal of attention. This attention is currently intensifying, as the technology demands thinner dielectric films of higher "quality" for submicron-scale integrated circuits.

It is desirable to include in this paper a section on the growth of SiO_2 films not only because of their technological importance just mentioned, but also because the current view of the growth mechanism is significantly different from those discussed so far. Recently, several articles have appeared in which the growth process has been discussed in considerable detail (Fair, 1981; Revesz and Schaeffer, 1982; Mott, 1981,1982). In this paper we will concentrate mainly on the processes by which reactants are transported across the film and the inconsistencies which exist in the current interpretation of the mechanism. The kinetic equation of Deal and Grove (1965) for oxidation in oxygen will first be presented, and the parabolic component of the kinetics will be analyzed in terms of diffusion processes within the oxide in order to compare and contrast the behavior with that of other oxides described in earlier sections. This will then be extended to the growth of thin films and finally to oxidation in steam.

A. Growth of thick SiO_2 films in O_2

The linear-parabolic equation used by Deal and Grove to describe the kinetics of SiO_2 growth takes the form

$$X^2+AX=B(t+t_0)\,, \tag{4.1}$$

where A and B are constants and t_0 accounts for the existence of a film even at $t=0$. There are conflicting reports in the literature concerning the lowest value of X for which this expression fits the experimental data. In their original paper Deal and Grove reported that this model gave a good fit to the observed oxidation kinetics in oxygen only for $X>30$ nm, and this was subsequently verified in the detailed studies of Irene and co-workers (Irene and Ghez, 1977; Irene and Van der Meulen, 1976). However, in a recent study, Lie *et al.* (1982) claim that the model is valid for $X>4$ nm when due account is taken of the initial transient conditions of the oxidation experiment. This discrepancy apart, the model has found widespread acceptance for describing the kinetics at temperatures >700 °C. For thin films ($X\ll A$) the growth kinetics are approximately linear and the rate constant is equal to B/A, i.e., $dX/dt=B/A$. For thick films ($X\gg A$) the kinetics tend to parabolic with a rate constant equal to B, i.e., $d(X^2)/dt=B$. The constant A, and hence the transition from thin to thick films, depends on temperature (see Fig. 20). Deal and Grove found that, for $a(O_2)<1$, both B and B/A are proportional to oxygen pressure, i.e., A independent of $a(O_2)$, and the activation energies are 1.24 and 2.0 eV, respectively.

Since B is identical to the parabolic rate constant k_p defined earlier, it is tempting to apply Wagner's theory to calculate B from tracer diffusion data using Eq. (2.5) and assuming SiO_2 is an electronic conductor. Since $D^*(O)\gg D^*(Si)$ in amorphous SiO_2 [e.g., Schaeffer (1980)], only oxygen transport need be considered and $D^*(O)$ has been measured by Williams (1965) to be proportional to $a(O_2)$ (Fig. 21). Equation (2.5) may thus be integrated (putting $f=1$) to give

$$B(O_2)=D^*(O)\,, \tag{4.2}$$

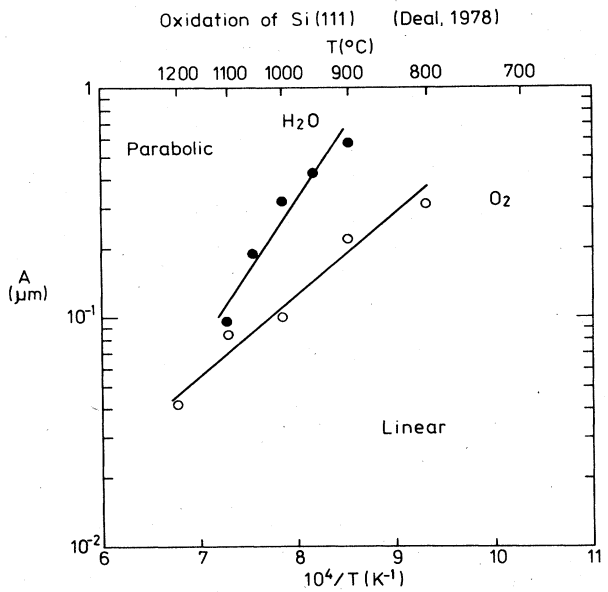

FIG. 20. Arrhenius plot of the parameter A of the kinetic model of Deal and Grove measured for the growth of SiO_2 on Si in O_2 or H_2O at a pressure of 1 atm. The growth kinetics are parabolic when the film is much thicker than A and linear when much less than A. The data are from Deal (1978).

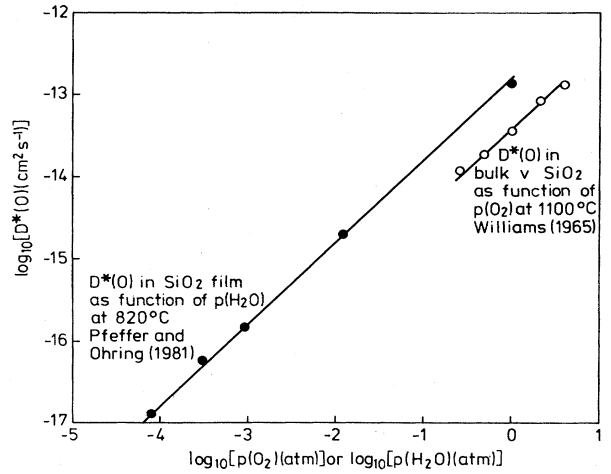

FIG. 21. Tracer self-diffusion coefficient for oxygen in bulk samples of amorphous SiO_2 as a function of oxygen pressure and in thermally grown SiO_2 films as a function of water vapor pressure.

where $D^*(O)$ is measured at the oxygen activity of the gas. Thus B is predicted to be proportional to $a(O_2)$, as observed, and the magnitude of $B(O_2)$ (see Fig. 22) is approximately correct. However, the observation that

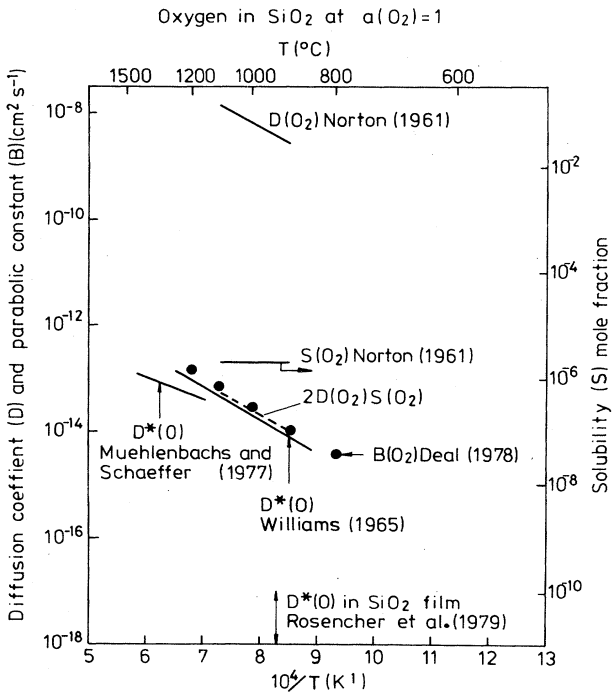

FIG. 22. Arrhenius plot of the parabolic rate constant measured by Deal (1978) for the growth of SiO_2 on Si in O_2 and other parameters relevant to the transport of O in bulk amorphous SiO_2 and SiO_2 films. All data are for an oxygen pressure of 1 atm. If oxygen transport takes place by interstitially dissolved O_2 molecules which exchange freely with network oxygen, then $B=2D(O_2)S(O_2)=2D^*(O)$.

$D^*(O)$ is proportional to $a(O_2)$ invalidates the application of Wagner's theory, because the only oxygen defect which can readily account for this proportionality is an uncharged interstitial O_2 molecule. Since this may diffuse without a coupled flow of electrons, Wagner's theory is not relevant and a simpler diffusion model may be used, as done by Deal and Grove. [In principle, charged defects such as O_2^- or V_{Si}'''' are possibilities, but to give a linear dependence on $a(O_2)$ would then require SiO_2 to be a good electronic conductor, which is unlikely.]

In Deal and Grove's atomistic interpretation of their kinetic model the parabolic rate constant is given by

$$B(O_2)=2D(O_2)S(O_2)\ , \tag{4.3}$$

where $D(O_2)$ is the diffusion coefficient of interstitial oxygen molecules and $S(O_2)$ is their concentration, or solubility (in mole fraction), at the oxide/gas interface. $D(O_2)$ is independent of $a(O_2)$, whereas $S(O_2)\propto a(O_2)$. Equation (4.3) is analogous to that derived in the point defect description of thick film growth [e.g., Eq. (2.14)].

$D(O_2)$ should not be confused with the tracer diffusion coefficient $D^*(O)$. Indeed, if these same interstitial O_2 molecules are also the defects by which network oxygen diffuses [as they would have to be to account for $D^*(O)\propto a(O_2)$], then $D^*(O)=D(O_2)S(O_2)$ (Shaeffer, 1978), neglecting correlation effects, and

$$B(O_2)=2D^*(O)\ . \tag{4.4}$$

This differs by only a factor of 2 from Eq. (4.2), which resulted from the invalid application of Wagner's theory. $D^*(O)$ has also been measured by Muehlenbachs and Schaeffer (1977), and their data are in reasonable agreement with those of Williams. $D^*(O)$ and $B(O_2)$ are compared in Fig. 22 and illustrate the approximate validity of Eq. (4.4). Furthermore, values of $D(O_2)$ and $S(O_2)$ are available from Norton's (1961) measurements of oxygen permeation through bulk amorphous SiO_2, and these are also plotted in Fig. 22. When substituted into Eq. (4.3), these data also predict B in reasonable agreement with the measured values (see Fig. 22). Therefore, parabolic film growth, tracer diffusion, and permeability all appear self-consistent.

Unfortunately, the experiments of Rosencher *et al.* (1979) are not in accord with the above correlations. They grew SiO_2 films first in oxygen of normal isotopic abundance and then in oxygen enriched in ^{18}O. They found that 93% of the ^{18}O incorporated in the film had passed through that grown in the first stage, without exchanging with the ^{16}O in the SiO_2 network, and was incorporated at the Si/SiO_2 interface by the formation of new oxide. Only ~7% was located at the SiO/O_2 interface, and this could have been incorporated either by exchange or by the outward diffusion of Si. Had these experiments been consistent with the tracer measurements on bulk amorphous SiO_2, all the ^{18}O would have been incorporated by exchange at the outside of the film (see Fig. 8). By assuming that the small amount of ^{18}O actually observed to be incorporated near the SiO/O_2 interface is the result of diffusion-controlled exchange, Revesz and

Schaeffer (1982) have estimated that $D^*(O)$ must be 3—4 orders of magnitude lower in the film than in the bulk samples as shown in Fig. 22. There appear to be two possible explanations for this difference between the apparent properties of thermally grown and bulk amorphous SiO_2. The first is that the two are sufficiently different in structure that gaseous and interstitial O_2 do not exchange with network oxygen in films, but do in bulk. There are several reports in the literature of structural differences between films and bulk SiO_2. Gibson and Dong (1980), using transmission electron microscopy, have observed channel structures in films grown in oxygen. Taft (1978) reports that the refractive index of SiO_2 grown in oxygen is a function of temperature (for $T < 1100\,^\circ C$), is always greater than that of bulk samples, and corresponds to the film's having a higher density (by up to 3%) than the bulk oxide. Irene, Dong, and Zeto (1980) have measured the density of SiO_2 films to be in the range 2.26—2.45 $g\,cm^{-3}$, depending on growth conditions (cf. 2.20 for bulk amorphous SiO_2 and 2.65 for crystalline quartz). There is thus convincing evidence for the existence of structural differences, but no means of assessing whether these can account for the behavior of ^{18}O tracers. Irene (1982b) has attempted to gain further information on the diffusive properties of films by the interrupted growth, or Rosenberg (1960), technique, which should give $D(O_2)$ for the film. Unfortunately, $D(O_2)$ was found to be so rapid as to be unmeasurable by this technique, as expected from Norton's early experiments on bulk specimens. [Irene found some evidence for a lower than expected $D(O_2)$ at 1000 °C, but the effect is close to the limits of the experimental technique.] The second possible explanation of the ^{18}O experiments is that the rate of exchange between interstitial O_2 and network O is such that very little exchange could take place in the oxidation experiments, whereas much more occurred in the longer times of the diffusion experiments, with the structural differences having negligible influence. Whatever the explanation, further experiments will be required to resolve this problem. As a further complication, Mott (1982) has pointed out that to explain the dissolution of interstitial O_2 in SiO_2 the standard enthalpy change of the dissolution reaction must be very small [since $S(O_2)$ is independent of T, as shown in Fig. 22] and the distance between sites that have this low energy must be relatively large (~ 2.5 nm). Since direct jumps over such a distance are unlikely, Mott proposed that there are higher energy sites of closer spacing that control diffusion but not solubility. Despite this added complexity, it may be shown that if O_2 molecules in the two sets of sites are in equilibrium then the correlations referred to previously are still valid, but with $D(O_2)$ being an effective diffusion coefficient between the solubility sites.

The mechanism which has been discussed above is based on uncharged O_2 interstitial molecules being responsible for transport through the film. However, Jorgensen (1962) found that the growth rate could be accelerated or retarded by an applied electric potential and that the reaction stopped when the oxide/gas interface had a potential of 1.78 V with respect to the Si/SiO_2 interface. This is difficult to reconcile with the above mechanism. Mott (1982) has proposed that when (and only when) electrons are available through the external circuit, transport may take place by a charged defect, the electronic conductivity of SiO_2 being too low for electrons to form the charged defects at a significant rate under open circuit conditions. However, electrochemical experiments by Jorgensen (1967) and Mills and Kröger (1973) indicate that $t_{ion} \sim 0.5$ in both bulk and SiO_2 films. It is clear that to reconcile this behavior with the molecular transport model will require further experiments; oxygen tracer experiments under an applied electric field (and short-circuit conditions) would be particularly informative.

B. Growth of thin SiO_2 films in O_2

The growth of thin films can be divided into two regions, depending on temperature. When $T > 700\,^\circ C$, thin film growth is dominated by the linear term of the Deal-Grove equation (B/A) subject to the uncertainty referred to earlier concerning its application for films less than ~ 30 nm in thickness. In Deal and Grove's model the linear rate constant is given by

$$\frac{B}{A} = \frac{S(O_2)}{\frac{1}{h_1} + \frac{1}{h_2}}, \tag{4.5}$$

where h_1 and h_2 are first-order rate constants for the interfacial reactions. It is normally assumed that the reaction at the Si/SiO_2 interface is the slowest one, but this is not a necessary requirement of the model. Since $S(O_2)$ is proportional to $a(O_2)$ and h_1 and h_2 are independent of $a(O_2)$, B/A should be proportional to $a(O_2)$, as originally reported by Deal and Grove. However, Lie *et al.* (1982) have extended the pressure range up to 20 atm and found that although B is proportional to $a(O_2)$, B/A is approximately proportional to $a(O_2)^{3/4}$ as shown in Fig. 23. This observation supports the suggestions of Blanc (1978) and Ghez and van der Meulen (1972) of a substantial contribution from interstitial O atoms to the reaction at the Si/SiO_2 interface [for which the linear rate constant would then be predicted to be proportional to $a(O_2)^{1/2}$]. Blanc also concludes that when O atoms are included in the model the modified kinetic equation fits the data of Irene and co-workers down to thicknesses of 1 nm. Furthermore, Irene (1982a) has shown evidence of curvature in the Arrhenius plot for B/A which is consistent with both O and O_2's being oxidizing species at the Si surface. There is also some evidence that below about 800 °C further complications may arise which are related to the inability of the film to deform by viscous flow at low temperatures and a resulting buildup of compressive stress (Irene, 1982c).

The mean activation energy for B/A is high (2.0 eV) and for temperatures below $\sim 700\,^\circ C$ this interfacial reaction rate becomes so low that the growth rate by this

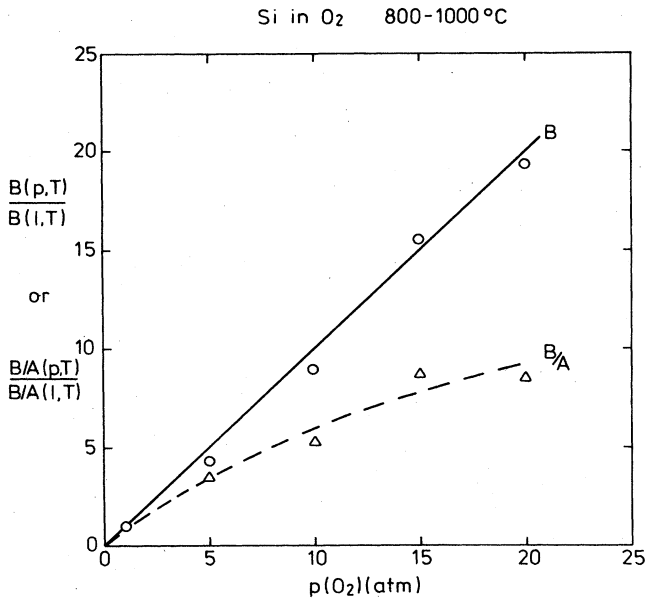

FIG. 23. Dependence of the parabolic rate constant (B) and the linear rate constant (B/A) on oxygen pressure for the growth of SiO_2 on Si in O_2 at temperatures in the range 800°C—1000°C. The data have been normalized to their values at an oxygen pressure of 1 atm (from Lie *et al.*, 1982).

mechanism becomes negligible in reasonable times (e.g., only 4×10^{-10} m in 24 h at 600°C). In Fig. 24 the rate of growth of thin SiO_2 films at 600°C and 400°C is plotted as a function of film thickness using data from Goodman and Breece (1970) and Fehlner (1972). As demonstrated by Fehlner, it is not possible to say whether direct or indirect logarithmic rate equations best describe the growth kinetics. Also shown in Fig. 24 are the linear and parabolic rates extrapolated from the data measured at higher temperatures. It can be seen that the growth rate is always faster than the linear rate, but slower than the parabolic rate. This is in marked contrast to other oxidation systems (e.g., Ni to NiO), where the low-temperature rate is always greater than the extrapolated parabolic rate. It can be concluded that even at 400°C the rate of diffusion of O_2 through the film is sufficiently rapid not to limit the SiO_2 growth rate. In addition, the presence of dissolved O_2 in the film means that electrons do not have to tunnel all the way to the SiO_2/O_2 interface in order to form oxygen ions, as envisaged in the Cabrera and Mott theory of thin-film growth. If this is the case, why are Cabrera-and-Mott—type kinetics observed? The explanation for this appears to reside in the low concentration of dissolved O_2 which is permitted in the film. If we assume that the electronic levels in dissolved ionized oxygen are the same as in adsorbed ionized surface oxygen then the equalization of electron energies by tunneling will be approximately as illustrated in Fig. 4 provided that the concentration of interstitial O_2 is very low. The shift in levels is usually ~1 eV. Now, the density of occupied solubility sites for dissolved O_2 in equilibrium with O_2 gas at 1 atm pressure is 5×10^{22} m^{-3} (Mott, 1981) and the spacing between these sites (counting both occupied and unoccupied) is ~2.5 nm. For a dielectric film of thickness X containing a uniform charge density ρ and on a metal substrate, the voltage drop across the dielectric is given by

$$\Delta\varphi=\frac{3\rho X^2}{\varepsilon\varepsilon_0}\ . \tag{4.6}$$

Thus for $X=5$ nm, $\varepsilon=10$, and $\rho=5\times10^{22}e/m^3$, $\Delta\varphi$ is only 7 mV. The conclusion is that for thin films the quantity of oxygen dissolved in the film is too low even when ionized to enable the electronic levels to be equilibrated and the space charge within the film remains negligible, as required by the Cabrera and Mott theory. As a result, the voltage is developed by charges in the Si and at the interfaces of the film. In the spirit of the Cabrera and Mott theory the rate-determining step in thin film growth should be the injection of a charged defect at one of the interfaces. The defect in the oxide responsible for film growth has therefore apparently changed from being a neutral interstitial O_2 molecule in thick films to a charged defect in thin films grown at temperatures below 700°C. This is similar to the change which appears to take place in a thick film when it is contacted by an external electrode.

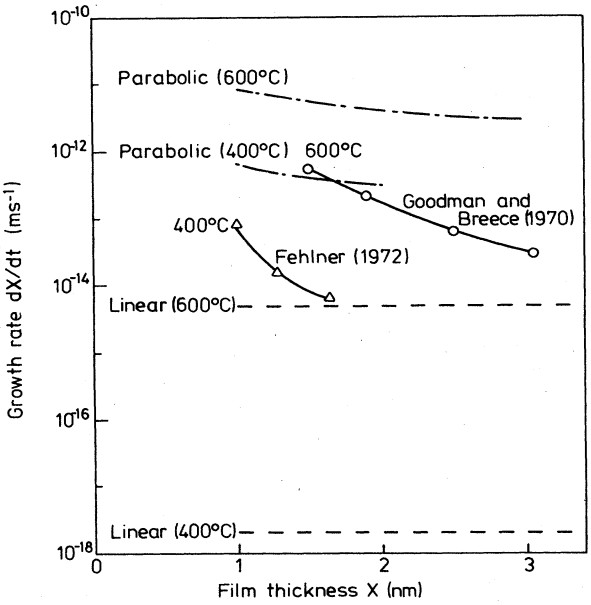

FIG. 24. Growth rate of SiO_2 films as a function of thickness on Si in O_2 in the "logarithmic" regime (temperatures below 700°C at a pressure of 1 atm). The broken curves are the parabolic and linear growth rates extrapolated from kinetic measurements at temperatures above 700°C.

C. Growth of thick SiO_2 films in H_2O

We shall now consider the oxidation of Si in water vapor. Water vapor, when present as an impurity in oxygen, has a substantial effect on the film-growth rate (Irene and Ghez, 1977), but the discussion here will be limited to oxi-

dation by water vapor in its own right. Returning to thick films and the Deal-Grove equation, it is found that in water vapor both the linear and parabolic rate constants are proportional to $p(H_2O)$, even over a large pressure range (Razouk *et al.*, 1981), and both are much greater than for oxygen. While the parabolic rate constant has a lower activation energy (0.71 eV) than for oxygen, that of the linear rate constant is almost the same (2.0 eV).

We can analyze the parabolic rate constant in the same way as for oxidation in oxygen, since the observed linear dependence on $p(H_2O)$ indicates that dissolved interstitial H_2O molecules are the diffusing species. Thus the equation analogous to Eq. (4.3) is

$$B(H_2O)=D(H_2O)S(H_2O) \tag{4.7}$$

(the factor 2 is missing, since one H_2O molecule supplies only one atom of oxygen to the silicon). We would expect $D(H_2O)$ to be independent of $p(H_2O)$, and $S(H_2O)$ to be proportional to $p(H_2O)$. However, the parameters $D(H_2O)$ and $S(H_2O)$ have not been measured in bulk amorphous SiO_2. This is because H_2O molecules react with network oxygen to form bound OH groups as typified by the reaction

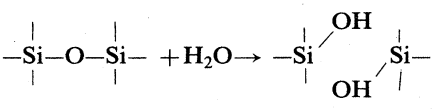

$$-\mathrm{Si}-\mathrm{O}-\mathrm{Si}- + \mathrm{H_2O} \rightarrow -\mathrm{Si}(\mathrm{OH})- \quad \mathrm{Si}(\mathrm{OH})- \tag{4.8}$$

The apparent diffusion coefficient, $D_{app}(OH)$, and the "solubility" $S(OH)$ of the OH groups have been measured by Moulson and Roberts (1961) by studying the reaction between H_2O vapor and amorphous SiO_2. They found that $S(OH)$ is proportional to $p(H_2O)^{1/2}$ as expected from Eq. (4.8). Doremus (1976) showed that the diffusion coefficients and solubilities are related by

$$D_{app}(OH)S(OH)=2D(H_2O)S(H_2O) . \tag{4.9}$$

Therefore $D_{app}(OH)$ should also be proportional to $p(H_2O)^{1/2}$. Moulson and Roberts assumed $D_{app}(OH)$ to be independent of $p(H_2O)$ in their analysis, but Doremus subsequently showed that their penetration profiles of OH were consistent with the expected $p(H_2O)^{1/2}$ dependence. The $D_{app}(OH)$ quoted by Moulson and Roberts is therefore approximately that appropriate to $p(H_2O)=1$ atm and their data are shown in Fig. 25. The expression for $B(H_2O)$ in terms of the measured parameters is

$$B(H_2O)=0.5D_{app}(OH)S(OH) , \tag{4.10}$$

and when Moulson and Roberts' data are substituted into this equation good agreement is found with the measured value of $B(H_2O)$ (see Fig. 25). Hence transport properties measured for "water" in bulk amorphous SiO_2 are in accord with the rate of growth of SiO_2 films in water vapor, and there is no evidence for a difference in behavior between the films and bulk specimens.

We shall now consider the behavior of tracers in diffusion and oxidation involving water. Two-stage $^{16}O_2/H_2{}^{18}O$ oxidation experiments, similar to the ones described earlier for pure oxygen, were carried out by Rigo *et al.* (1981). In contrast to the earlier results in pure O_2, Rigo *et al.* found that the ^{18}O from $H_2{}^{18}O$ exchanged with the network oxygen and was always located close to the SiO_2/gas interface. The ^{18}O penetration profile they observed at 930 °C and $p(H_2O)=13$ Torr corresponded to a diffusion coefficient of 5×10^{-15} cm^2 s^{-1}. If the oxygen in interstitial H_2O and the SiO_2 network can exchange freely, then we expect the tracer diffusion coefficient to be given by (neglecting correlation effects)

$$D^*(O,H_2O)=0.5D(H_2O)S(H_2O) , \tag{4.11}$$

and, therefore, from Eq. (4.7),

$$B(H_2O)=2D^*(O,H_2O) . \tag{4.12}$$

Assuming a linear dependence on $p(H_2O)$, the measurement of $D^*(O,H_2O)$ by Rigo *et al.* has been corrected to $p(H_2O)=1$ atm and is shown plotted in Fig. 25. The relationship with $B(H_2O)$ is in accord with Eq. (4.12). Rigo *et al.* deduced, however, that at 600 °C, the exchange between interstitial H_2O and network O was sufficiently sluggish to perturb the tracer penetration profiles.

Pfeffer and Ohring (1981) carried out similar studies but introduced O tracer by ion implantation into the SiO_2 network rather than via the gas phase. They observed the broadening of the ^{18}O depth profile due to exchange and diffusion when the film was subsequently annealed in atmospheres having different $p(H_2O)$. They verified that $D^*(O,H_2O)$ is proportional to $p(H_2O)$, as expected from Eq. (4.11), and as shown in Fig. 21. At $p(H_2O)=1$ atm they determined $D^*(O,H_2O)$ in the temperature range 260 °C—800 °C. When these data are extrapolated to the temperature range in which $B(H_2O)$ has been measured (see Fig. 25), they also are reasonably consistent with Eq. (4.12). However, in contrast to the findings of Rigo

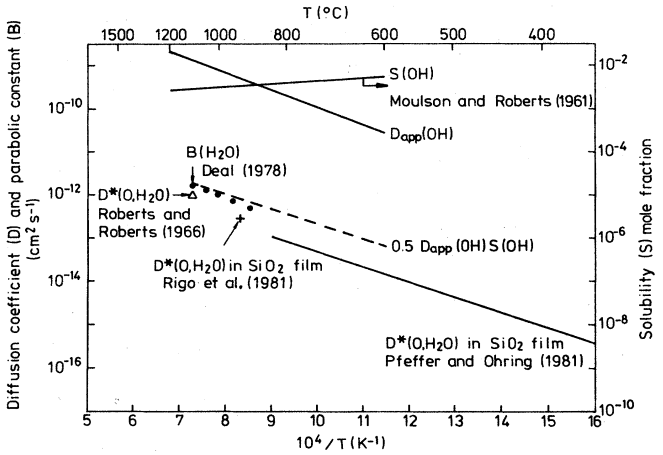

FIG. 25. Arrhenius plot of the parabolic rate constant measured by Deal (1978) for the growth of SiO_2 on Si in H_2O at a pressure of 1 atm. Data for other parameters relevant to the transport of oxygen in bulk amorphous SiO_2 and SiO_2 films in the presence of water vapor are also shown. If oxygen transport is by interstitially dissolved H_2O molecules which exchange oxygen freely with network oxygen, then $B=0.5D_{app}(OH)S(OH)=2D^*(O,H_2O)$.

et al., the results of Pfeffer and Ohring do not show evidence of sluggish exchange between interstitial H_2O and network oxygen even at temperatures below 600 °C.

Roberts and Roberts (1966) studied the reaction of $H_2{}^{18}O$ water vapor with bulk amorphous SiO_2. They found that the depth of ^{18}O penetration was much smaller than that of the incorporated OH groups, thereby indicating ready exchange between lattice oxygen and the oxygen in interstitial H_2O molecules. At the maximum temperature of their experiments (1100 °C) they estimate that $D^*(O,H_2O) \sim 10^{-12}$ cm^2 s^{-1} at $p(H_2O) \sim 1$ atm. This is also shown plotted in Fig. 25 and is reasonably consistent with the other tracer measurements.

None of the tracer measurements described in this section was in a system in chemical equilibrium. Therefore, they can be regarded as only approximations to the true tracer diffusion coefficient. Nevertheless, they are sufficient for us to conclude that the behavior of tracers in both bulk SiO_2 and in films is quantitatively consistent with other bulk transport properties and the parabolic rate constant for oxidation in H_2O. They confirm an atomistic picture of H_2O interstitial molecules diffusing through SiO_2 and exchanging oxygen not only with bound OH groups but also with network oxygen.

V. DUPLEX AND LATERAL FILM GROWTH

The film growth processes that we have considered thus far have assumed the film to be uniform and compact and to be growing at one of its external surfaces by the solid-state diffusion of reactants across it. In this section we will discuss two growth processes which deviate from this ideal. They are found in the growth of films of the oxides which were discussed in Sec. III. However, the occurrence of duplex and lateral film growth does not invalidate the analysis of film growth which was applied to these oxides in Sec. III, since they appear to be secondary processes. They do not occur under all conditions and they do not result in growth rates which are greatly different from those of growth by the conventional process. Nevertheless, they have important consequences for the microstructure of the film and its adherence to the metal substrate. They are phenomena which have been observed only in the thick film growth regime.

A. Growth of duplex films

A duplex film is a film that consists of two well-defined layers parallel to the metal substrate. In the case of films grown on alloys, or metals of low purity, the two layers usually have different chemical composition. In the case of pure metals the two layers, both of the same crystalline phase, differ in their microstructure. In early work on this subject the inner layer was reported to be porous and it has been assumed thereafter that the inner layer is always porous. However, recent investigations using transmission electron microscopy [e.g., Moseley *et al.* (1982) and Rowlands and Manning (1983)] have shown that the inner layer is not greatly porous and that many reports of porosity may possibly be ascribed to the plucking out of oxide grains during metallographic preparation. The general structure of a duplex film is shown in Fig. 26(a). The outer layer is columnar in structure, whereas the inner layer is much finer grained and the grains are equiaxed. The ratio of thickness of the two layers is, in general, variable. However, in many cases the boundary between the two layers is found to be coincident with the original position of the unoxidized metal surface (e.g., Atkinson and Taylor, 1982).

The conditions that favor the growth of duplex films are not particularly clear, but from their wide occurrence some generalizations can be made. Duplex films occur only in those oxides which are normally expected to grow by the outward diffusion of metal ions. They are com-

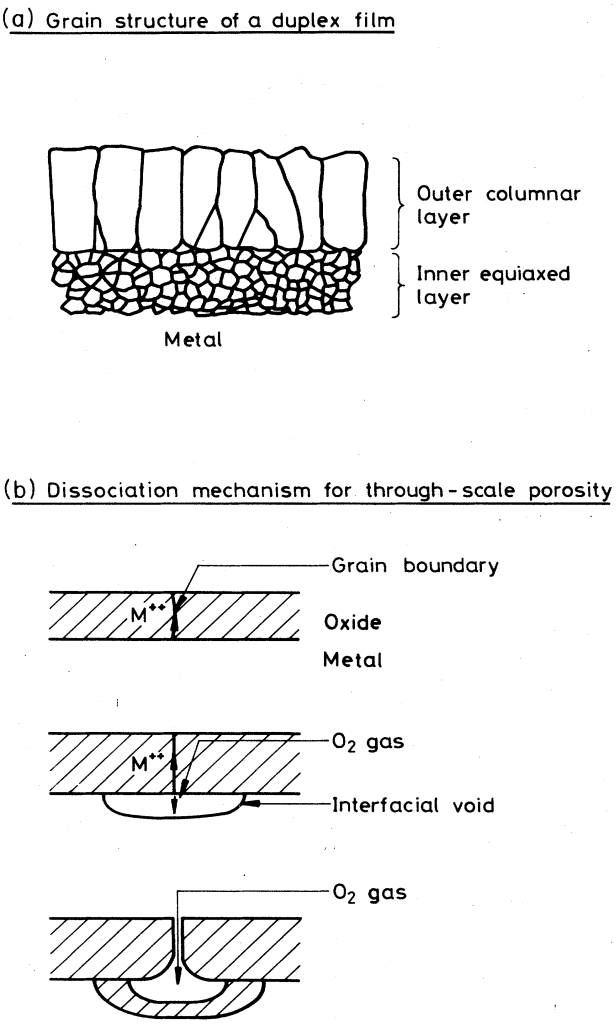

FIG. 26. (a) Schematic diagram showing the typical grain structure of a duplex oxide film. (b) The mechanism suggested by Mrowec (1967) for the formation of channels traversing the oxide film. Dissociation of the oxide is postulated to occur at oxide grain boundaries in regions of the film where the metal/oxide interface is separated.

monly found when the metal is impure or deliberately alloyed. For example, Atkinson and Taylor (1982) found that the addition of only 0.1% by weight of Si to Fe was sufficient to cause the Fe_3O_4 film to grow in a duplex structure at 500 °C. The occurrence of the duplex structure is also dependent on the structure of the substrate. For example, Atkinson *et al.* (1979) observed that at 1000 °C a single-layer film grew on {100} orientation Ni single crystals, whereas a duplex film grew on polycrystalline Ni under the same conditions. Temperature is also a key variable, but its effect on whether a duplex film is formed is not clear. This is probably because there are two processes which can initiate duplex film growth, which will be described subsequently.

There have now been many investigations of duplex growth in a variety of oxides using the sequential $^{16}O/^{18}O$ oxidation technique to study the transport properties. These have been carried out for CoO (Sheasby and Brown, 1978), NiO (Atkinson *et al.*, 1979), Fe_3O_4 (Atkinson and Taylor, 1982; Gleave *et al.*, 1982a,1982b), and $Fe_3O_4/FeCr_2O_4$ (Taylor *et al.*, 1980; Pritchard *et al.*, 1980). Although differing in detail, all these investigations show the same general behavior. The final distribution of ^{18}O is consistent with the outer layer of the film's growing by the outward diffusion of metal ions while the inner layer grows by the inward short-circuit transport of oxygen. How is the oxygen transported inwards through the oxide? This could conceivably be by grain boundary diffusion, but this can be discounted for two reasons. The first is that the single-layered films also contain grain boundaries, but they show no inward penetration of oxygen during film growth. The second is that recent tracer measurements of diffusion of O along NiO grain boundaries (Fig. 12) show that it is too slow to account for inner-layer growth on Ni. All available evidence points to the direct penetration of the film by gas molecules when duplex films are growing. For example, Pritchard *et al.* (1975) found ^{14}C in the inner layer of duplex Fe_3O_4 films when a second oxidation stage was carried out in $^{14}CO_2$. However, the pathways along which the oxygen molecules are transported across the two layers are difficult to identify. Voids are always observed in oxide films, but it is difficult to establish their continuity. Hussey and Graham (1981) have studied the continuity of voids in Fe_3O_4 duplex films by serial polishing, and they concluded that none of the voids was part of a pore traversing the outer layer. However, the inner layer was thin in their experiments and ^{18}O tracers (Atkinson and Taylor, 1982) indicate that the inner layer in this case does not grow by inward diffusion of gas. Gleave *et al.* (1982) have observed pores by scanning electron microscopy of Fe_3O_4 outer layers grown in CO_2, which are probably continuous across the layer.

On the basis of these experimental findings we will now consider the probable mechanisms of duplex film growth. It would appear that there are three distinct varieties of duplex structure and growth. The first kind are the relatively thin inner layers ($<20\%$ total film thickness) which sometimes form on pure metals, such as the one just described in the case of Fe_3O_4. These do not grow by inward gas diffusion and in this respect are different from the other duplex films. The second kind are duplex structures formed in fast-growing oxides (e.g., FeO or some other oxides at very high temperature). In these cases a large fraction of the metal core is consumed and the origin of the duplex structure is almost certainly due to the problems of maintaining contact with the shrinking core, especially at specimen corners. The third kind are in slow-growing oxides (NiO, Fe_3O_4) on plane specimens where maintaining contact is not a problem and where the origin of the effect is "local."

In all cases, the dissociation processes considered by Mrowec and co-workers probably have some role to play, and therefore these will be briefly described. The mechanism was originally postulated to explain the formation of a duplex structure during the sulfidation of Fe. The basic idea is that if for some reason contact is lost between the metal and the film at their interface, the oxide above the detached area still has a gradient of chemical potential across it and (for the oxides which show duplex growth) metal ions will continue to migrate outwards. Since the metal cannot supply metal ions to the base of the film, the metal chemical potential there falls and $a(O_2)$ rises. Thus the oxide dissociates, sending metal ions outwards through the film and oxygen as gas into the void space, and the oxygen is available for further oxidation of the metal substrate. Unfortunately, the tracer experiments of Brückman and Romanski (1965) showed that, as in the later studies of oxides, the inner layers of FeS grew by the direct penetration of S_2 molecules. The simple dissociation mechanism was then modified by Mrowec (1967) to become a mechanism by which pores could be created traversing the oxide film and allowing the inward transport of gas. Mrowec proposed that rapid diffusion along oxide grain boundaries results in preferential dissociation along the boundaries and extending up to the oxide/gas interface, as illustrated in Fig. 26(b). In support of this, Raynaud, Clark, and Rapp (1984) have recently observed pores develop *in situ* in Cu_2O films on the outer surface of the oxide, using a scanning electron microscope with an environmental hot stage. If this really is the mechanism for creating gaseous diffusion paths, then the critical process which initiates duplex growth is detachment at the metal/oxide interface. For the fast-growing oxides this is probably a mechanical detachment due to lack of plasticity in the oxide. In the case of the slow-growing oxides on plane surfaces this cannot be the reason and it is more likely that detachment occurs by the nucleation of an interfacial void from point defect (vacancy) accumulation at the interface. This goes some way to accounting for the sensitivity of the phenomenon to impurities (which, when insoluble in the oxide, will accumulate at the interface) and metal crystallography and the fact that films thinner than $\sim 1\ \mu m$ do not normally show inward penetration of gas (Atkinson and Taylor, 1982).

Once a pore traversing the film has been created, the next question is "Is it stable or does it heal up?" It is possible to show that, by adjusting its cross-sectional area as

a function of position through the film, a pore can be stable with respect to sideways closure (Gibbs, 1973). However, we would always expect it to heal from the bottom upwards by the growth of new oxide as illustrated in Fig. 26. This would also partially explain why new inner-layer growth is not confined to the metal/inner-layer interface, but is usually distributed through the inner layer. Therefore, the pores must have a transient existence—old pores seal off and new ones are opened. Furthermore, the volume of oxide in the inner layer according to this mechanism is approximately equal to the integrated volume of the interfacial porosity, which, in turn, cannot exceed the volume of metal which has diffused outwards. Thus this mechanism provides an automatic coupling of the inner-layer growth rate to diffusion of metal ions across the total thickness of the film.

In summary, it appears that in nearly all cases of well-developed duplex films the inner layer grows by inward gaseous transport along fissures probably created by dissociation at oxide grain boundaries and initiated by loss of contact at the metal/oxide interface.

While this mechanism of duplex film growth is mainly qualitative and speculative, it does account for most of the experimental observations and is the best one currently available.

B. Lateral film growth

When both metal and oxygen species are mobile in the film (by solid-state diffusion), it is generally not necessary that each species migrates to the opposite boundary of the film for it to enlarge the film with a new unit of oxide. There exists the possibility that new oxide unit cells can be grown inside the film, at sites such as dislocations or grain boundaries, from the counterflow of species. If this internal growth takes place on planes parallel to the film boundaries, it will be indistinguishable from normal growth at the boundaries themselves. However, if the internal growth is on planes with a component perpendicular to the film boundaries, then the film will grow laterally with observable consequences. There are two types of observation from which the occurrence of lateral growth is generally inferred.

The first is the development of a compressive stress in the oxide which may cause elongation (creep) of the metal substrate. This effect has been reported to occur in the growth of NiO on Ni (Rhines and Wolf, 1970; Ueno, 1975) and in the growth of Cr_2O_3 on stainless steels (Harris, 1978). In these cases the actual quantity of lateral growth is small. The second observation is the development of highly convoluted films detached from the metal substrate, as illustrated in Fig. 27(a). This has been reported by many workers for the growth of Cr_2O_3 and Al_2O_3 films under some conditions [see, for example, summaries by Lillerud and Kofstad (1983); Hindam and Whittle (1983); and Wood and Stott (1983)]. In some instances the convoluted morphology represents a very large amount of lateral growth. Referring to Fig. 27(a), we see

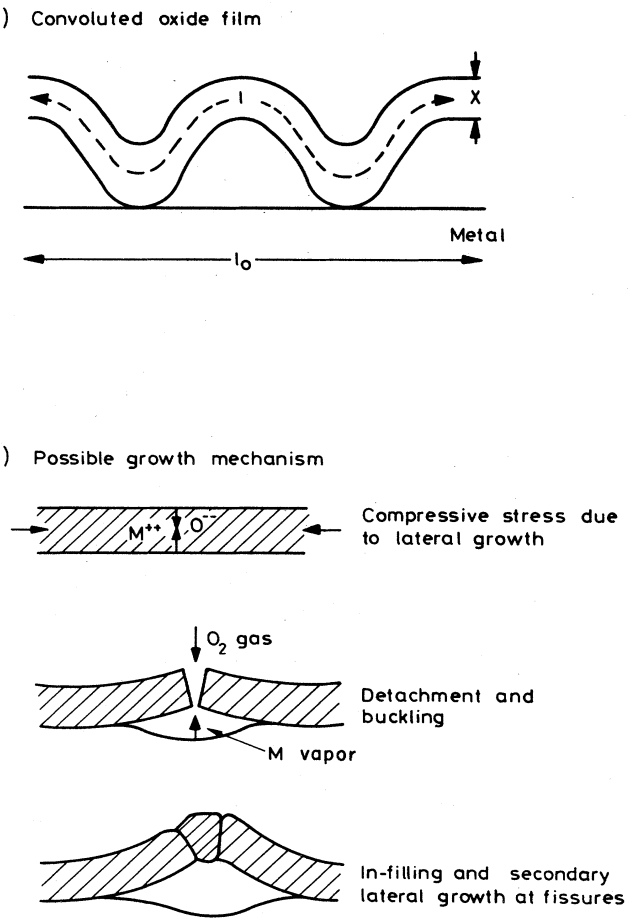

FIG. 27. (a) Schematic diagram of a highly convoluted oxide film which is sometimes observed in the growth of Cr_2O_3 and Al_2O_3. (b) A possible mechanism for the growth of convoluted films. In regions where the metal/oxide interface is separated the film buckles under the influence of compressive stress generated by lateral growth within the film.

that the volume of lateral oxide is $(l^2-l_0^2)X$ and that the volume of "normal" oxide is l_0^2X. Therefore, the ratio of lateral growth to "normal" growth is $(l/l_0)^2-1$. For a convoluted film this may be as large as a factor of 4.

Rhines and Wolf (1970) suggested that growth of NiO takes place by the reaction of Ni diffusing outward through the lattice with O diffusing inward along grain boundaries. Although this subsequently has been shown not to be the major process in NiO growth (for which Ni grain boundary diffusion is dominant at temperatures below 1100 °C, Sec. II.B, and Ni lattice diffusion at higher temperatures), a similar process could be responsible for the small amounts of lateral growth in NiO, and the mechanism is often quoted to explain lateral growth in Cr_2O_3 and Al_2O_3. However, it is not necessary to postulate that the reactants follow different reaction paths in order to have growth within the film. New oxide may be formed internally under certain circumstances from the usual counter diffusion of point defects.

Atkinson (1982) has used the point defect description of thick-film growth (following Kröger) to examine under what conditions the point defect fluxes will react to give new oxide within the film. The basis of the mechanism is that the condition of local chemical equilibrium is in general not compatible with the *individual* particle currents' being constant (although the equivalent sum is constant). The resulting divergence in the particle currents corresponds to the formation of new oxide within the film by defect reactions such as the Schottky reaction

$$(\mathrm{MO}) \rightarrow V_M'' + V_O^{\cdot\cdot} + (\mathrm{MO}) , \tag{5.1}$$

in which a new pair of oxide sites is created (growth). However, if the reaction is in the reverse sense, then vacancies are annihilated and the oxide lattice is consumed internally so that the film shrinks, or voids are produced. Reactions such as (5.1) can occur in an oxide film either at dislocations or grain boundaries, or by the nucleation of dislocation loops. Whenever these have a component perpendicular to the surface, lateral growth (or shrinkage) will be the result. For cases in which one species is dominant (e.g., the Ni vacancy in NiO) the transport equations can be solved to predict whether internal growth or consumption of oxide will occur (Table I). The predictions depend on the nature of the majority and minority defects and, since point defects are also believed to exist in grain boundaries and dislocations, should also be valid when transport is mainly along such short-circuit paths. Table I predicts that lateral growth will occur only if both defects are interstitials or if one is an uncharged interstitial and the other is a charged vacancy. Thus for NiO in which Ni vacancies are charged, lateral growth would imply oxygen diffusion by an uncharged interstitial O atom. It is not unreasonable that this may be the defect responsible for O diffusion in NiO grain boundaries and, at 1000 °C, would lead us to expect a lateral growth of $\sim 0.1\%$ (referring to Fig. 12) and be sufficient to explain the compressive stress inferred from experiments.

In the case of Cr_2O_3 there may well be both Cr vacancies and interstitials as majority defects depending on $a(O_2)$ (see Sec. III.D). This means there may be a changeover from vacancies to interstitials as the metal/oxide interface is approached, and the analysis would consequently be more difficult. However, inspection of Table I shows that the presence of cation interstitials makes internal growth very likely. The amount of internal growth, as in the case of NiO, cannot exceed that permitted by inward oxygen diffusion. Mitchell *et al.* (1983) estimate from ^{18}O tracer measurements at 700 °C that there is detectable oxygen diffusion in Cr_2O_3 films, but it is slower than Cr diffusion by "orders of magnitude." Indeed, their films did not grow in a convoluted geometry.

It would therefore appear that internal lateral scale growth by normal solid-state diffusion and point defect reactions is a possible explanation for compressive stresses which develop in growing films of NiO, Cr_2O_3, and Al_2O_3 on plane substrates. However, what little evidence is available in Cr_2O_3 suggests that this is not the mechanism for the large amount of lateral growth in the highly convoluted films of Cr_2O_3 and Al_2O_3 which sometimes form, because the current of minority species is too small. It would therefore appear that highly convoluted film growth is a secondary process which follows an initial separation of the film from the substrate either by point-defect aggregation at the metal/oxide interface, or as a response to stresses induced by a small amount of lateral growth. For metals having a low vapor pressure, dissociation and duplex film growth follow as described in the preceding section. For metals such as Al and Cr which have a high vapor pressure, dissociation will not occur (because metal is supplied to the film as a vapor), and the unsupported film can grow in a nonplanar manner, as illustrated speculatively in Fig. 26(b).

VI. SUMMARY AND CONCLUSIONS

We have surveyed the current status of theory for the growth of both thick and thin oxide films and how well they can account for the measured rates of growth of a variety of examples in terms of what is known about the transport properties of the oxides. There are inevitably many topics that have not been considered here, such as the growth of solid-solution (doped) films and the complex interplay of diffusion and thermodynamics which controls film growth on alloys. Nevertheless, the topics that have been covered should serve as a good representation of the variety of processes that can participate in film growth and our current appreciation of them.

The theories of Wagner for thick films and Cabrera and Mott for thin films have been used as a basis for interpreting experimental observations. The Wagner theory

TABLE I. Conditions for internal growth according to the type of defect pair. +, oxide formation. −, oxide consumption. 0, neither formation nor consumption.

Minority defect	Majority defect			
	Charged vacancy $V_m^{\cdot\cdot}$	Uncharged vacancy V_m^x	Charged interstitial $M_i^{\cdot\cdot}$	Uncharged interstitial M_i^x
charged vacancy $V_O^{\cdot\cdot}$	−	−	0	+
uncharged vacancy V_O^x	−	−	−	0
charged interstitial $O_i^{\cdot\cdot}$	0	−	+	+
uncharged interstitial O_i^x	+	0	+	+

is readily compared with experiment, and the agreement is good for fast-growing oxides and at relatively high temperatures, e.g., for CoO. At intermediate temperatures the growth rate predicted from lattice diffusion and the Wagner theory is usually several orders of magnitude slower than is actually observed (e.g., NiO, Fe_3O_4, Cr_2O_3, and Al_2O_3). In the case of NiO the diffusion of Ni along NiO grain boundaries has been shown to be responsible for the faster growth rate. When the Wagner theory is modified to include grain boundary diffusion, it can explain the growth of NiO films for all temperatures above 300 °C and for all films thicker than 30 nm. By inference, similar behavior is expected in Fe_3O_4, Cr_2O_3, and Al_2O_3 (and all crystalline oxides at sufficiently low temperature), but the diffusion data required to test out this hypothesis are not available. The point defects responsible for lattice diffusion are reasonably well understood for CoO, NiO, and Fe_3O_4, and significant improvements are being made in understanding point defects in Cr_2O_3. Films of all these oxides grow by outward metal diffusion. Point defects in Al_2O_3 stubbornly resist understanding because of the sensitivity of the defect properties to trace impurities. However, all available evidence points to the inward diffusion of oxygen along Al_2O_3 grain boundaries as being the dominant transport process in Al_2O_3 growth. Given the overall importance of boundary diffusion, a significant gap in current understanding is lack of a theory to predict the grain size in a growing film.

Thin film growth is not so well understood as thick film growth, and the Cabrera and Mott theory contains parameters that cannot be determined in independent measurements. Although the Cabrera and Mott theory qualitatively explains many observations, there are also many anomalies. For example, in the growth of thin films of NiO, the effect of an applied electric field is not consistent with the theory. Also, the growth of thin Al_2O_3 films appears to be controlled by the outward diffusion of Al, in contrast to the inward diffusion of O which controls thick film growth. Cr_2O_3 is the only oxide for which a single transport process (outward diffusion of Cr along Cr_2O_3 grain boundaries) is capable of satisfactorily explaining both thick and thin film growth (although a similar situation may also exist for NiO). Thin film growth has been a neglected area in recent years and is probably worthy of more effort.

The growth of SiO_2 films is significantly different from the other examples, because they are amorphous (and therefore grain boundary diffusion is not possible), and because the reaction at the Si/SiO_2 interface is relatively slow. The kinetics are satisfactorily described by a reaction model (Deal and Grove, 1965) involving diffusion transport and interfacial reaction, except for relatively thin films (<30 nm) grown in O_2. The available data for the parabolic growth of SiO_2 films in O_2 and H_2O, tracer diffusion of O, solubility of O_2 and OH, and their diffusion coefficients can all be reconciled, except for the tracer diffusion of O in SiO_2 films grown in O_2. (Further experiments of O tracer diffusion in bulk SiO_2 and SiO_2 films will be necessary to resolve this discrepancy.) Most of the experimental observations can be successfully correlated by assuming that the diffusing species are electrically neutral interstitial O_2 and H_2O molecules. However, some observations which indicate charged species cannot be reconciled with this picture at present. The interfacial component of the overall reaction is not well understood. Very thin (<5 nm) SiO_2 films appear to grow by the Cabrera and Mott mechanism. Since this requires a charged species, it is not clear how this relates to the growth of thicker films by neutral species.

Finally, our understanding of more intricate film-growth mechanisms, such as duplex and lateral film growth, is at a very rudimentary level. It has been established that duplex film growth is a secondary process in films which normally grow by outward metal diffusion. The inner layer of the duplex structure almost always grows by inward penetration of gaseous oxygen, or oxygen-bearing species. However, the conditions for duplex growth have never been well defined in a single system, and the most probable mechanism by which the gaseous diffusion paths are created remains speculative. Small quantities of lateral growth can be understood in terms of an extension of the theory of thick film growth to include internal growth from metal and oxygen countercurrents. The theory predicts that only certain combinations of point defects are capable of producing lateral growth. However, knowledge of point defects, particularly in grain boundaries, is not sufficiently well developed to test the theory. Although this probably accounts for the generation of compressive stresses in growing films, it seems unlikely that it can account for the large quantities of lateral growth that occur in the formation of highly convoluted films.

It is clear that even for the growth of simple oxide films on simple metal (or semiconductor) substrates there is much that remains to be understood.

ACKNOWLEDGMENTS

I would like to thank P. W. Tasker for many useful discussions and A. E. Hughes for his comments on the manuscript.

REFERENCES

Atkinson, A., 1982, Corros. Sci. **22**, 347.
Atkinson, A., A. E. Hughes and A. Hammou, 1981, Philos. Mag. A **43**, 1071.
Atkinson, A., F. C. W. Pummery, and C. Monty, 1985, "Diffusion of ^{18}O tracer in NiO grain boundaries" in Proceedings of 3rd International Conference on Transport in Non-Stoichiometric Compounds, Pennsylvania State University (to be published).
Atkinson, A., and R. I. Taylor, 1979, Philos. Mag. A **39**, 581.
Atkinson, A., and R. I. Taylor, 1981, Philos. Mag. A **43**, 979.
Atkinson, A., and R. I. Taylor, 1982, High Temp. High Pressures **14**, 571.
Atkinson, A., and R. I. Taylor, 1983, J. Mater. Sci. **18**, 2371.

Atkinson, A., and R. I. Taylor, 1985, "Diffusion of ^{51}Cr tracer in Cr_2O_3 and the growth of Cr_2O_3 films" in Proceedings of 3rd International Conference on Transport in Non-Stoichiometric Compounds, Pennsylvania State University (to be published).
Atkinson, A., R. I. Taylor, and P. D. Goode, 1979, Oxid. Met. **13**, 519.
Atkinson, A., R. I. Taylor, and A. E. Hughes, 1982, Philos. Mag. A **45**, 823.
Barnes, D. G., J. M. Calvert, K. A. Hay, and D. G. Lees, 1973, Philos. Mag. **28**, 1303.
Berry, L., and J. Paidassi, 1966, C. R. Acad. Sci. **262**, C-1353.
Blanc, J., 1978, Appl. Phys. Lett. **33**, 424.
Boggs, W. E., R. H. Kachik, and G. E. Pellissier, 1965, J. Electrochem. Soc. **112**, 539.
Brückman, A., and J. Romanski, 1965, Corros. Sci. **5**, 185.
Cabrera, N., and N. F. Mott, 1949, Rep. Prog. Phys. **12**, 163.
Caplan, D., and M. Cohen, 1966, Corros. Sci. **6**, 321.
Caplan, D., M. J. Graham, and M. Cohen, 1972, J. Electrochem. Soc. **119**, 1205.
Caplan, D., and G. I. Sproule, 1975, Oxid. Met. **9**, 5.
Caplan, D., G. I. Sproule, R. J. Hussey, and M. J. Graham, 1978, Oxid. Met. **12**, 67.
Catlow, C. R. A., W. C. Mackrodt, M. J. Norgett, and A. M. Stoneham, 1979, Philos. Mag. A **40**, 161.
Channing, D. A., and M. J. Graham, 1972, Corros. Sci. **12**, 271.
Chen, W. K., and R. A. Jackson, 1969, J. Phys. Chem. Solids **30**, 1309.
Chen, W. K., and N. L. Peterson, 1975, J. Phys. Chem. Solids **36**, 1097.
Davies, D. E., U. R. Evans, and J. N. Agar, 1954, Proc. R. Soc. London Ser. A **225**, 443.
Deal, B. E., 1978, J. Electrochem. Soc. **125**, 576.
Deal, B. E., and A. S. Grove, 1965, J. Appl. Phys. **36**, 3770.
Dieckmann, R., 1977, Z. Phys. Chem. Neue Folge **107**, 189.
Dieckmann, R., 1984, Solid State Ionics **12**, 1.
Dieckmann, R., and H. Schmalzried, 1977, Ber. Bunsenges. Phys. Chem. **81**, 414.
Dignam, M. J., D. J. Young, and D. G. W. Goad, 1973, J. Phys. Chem. Solids **34**, 1227.
Doremus, R. H., 1976, J. Phys. Chem. **80**, 1773.
Dubois, C., C. Monty, and J. Philibert, 1982, Philos. Mag. **46**, 419.
Fair, R. B., 1981, in *Silicon Integrated Circuits,* edited by D. Kahng, Applied Solid State Science, Supplement 2B (Academic, New York), pp. 1—108.
Fehlner, F. P., 1972, J. Electrochem. Soc. **119**, 1723.
Fehlner, F. P., 1984, J. Electrochem. Soc. **131**, 1645.
Francis, R., and D. G. Lees, 1976, Corros. Sci. **16**, 847.
Fromhold, A. T., 1976, *Theory of Metal Oxidation—Volume 1, Fundamentals,* Defects in Crystalline Solids (North-Holland, Amsterdam), Vol. 9.
Fromhold, A. T., 1979, J. Phys. Soc. Jpn. **48**, 2022.
Fromhold, A. T., 1980, *Theory of Metal Oxidation—Volume 2, Space Charge,* Defects in Solids (North-Holland, Amsterdam), Vol. 12.
Fueki, K., and J. B. Wagner, 1965, J. Electrochem. Soc. **112**, 384.
Garnaud, G., and R. A. Rapp, 1977, Oxid. Met. **11**, 193.
Gesmundo, F., and F. Viani, 1981, J. Electrochem. Soc. **128**, 460.
Gesmundo, F., and F. Viani, 1982, Solid State Ionics **6**, 33.
Ghez, R., 1973, J. Chem. Phys. **58**, 1838.
Ghez, R., and Y. J. van der Meulen, 1972, J. Electrochem. Soc. **119**, 1100.
Gibbs, G. B., 1973, Oxid. Met. **7**, 173.
Gibson, J. M., and D. Dong, 1980, J. Electrochem. Soc. **127**, 2722.
Gleave, C., J. M. Calvert, D. G. Lees, and P. C. Rowlands, 1982a, Proc. R. Soc. London Ser. A **379**, 409.
Gleave, C., J. M. Calvert, D. G. Lees, and P. C. Rowlands, 1982b, Proc. R. Soc. London Ser. A **379**, 429.
Goodman, A. M., and J. M. Breece, 1970, J. Electrochem. Soc. **117**, 982.
Goursat, A. G., and W. W. Smeltzer, 1973, Oxid. Met. **6**, 101.
Graham, M. J., and M. Cohen, 1972, J. Electrochem. Soc. **119**, 879.
Grimley, T. B., 1955, in *Chemistry of the Solid State,* edited by W. E. Garner (Butterworths, London), p. 336.
Himmel, L., R. F. Mehl, and C. E. Birchenall, 1953, Trans. Am. Inst. Min. Eng. **197**, 827.
Hindam, H., and D. P. Whittle, 1983, Oxid. Met. **18**, 245.
Hoshino, K., and N. L. Peterson, 1983, J. Am. Ceram. Soc. **66**, C-202.
Hagel, W. C., and A. U. Seybolt, 1961, J. Electrochem. Soc. **108**, 1146.
Hope, G. A., and I. M. Ritchie, 1976, Thin Solid Films **34**, 111.
Hunt, G. L., and I. M. Ritchie, 1970, Oxid. Met. **2**, 361.
Hussey, R. J., D. Caplan, and M. J. Graham, 1981, Oxid. Met. **15**, 421.
Hussey, R. J., and M. J. Graham, 1981, Corros. Sci. **21**, 255.
Hussey, R. J., G. I. Sproule, D. Caplan, and M. J. Graham, 1977, Oxid. Met. **11**, 67.
Irene, E. A., 1982a, Appl. Phys. Lett. **40**, 74.
Irene, E. A., 1982b, J. Electrochem. Soc. **129**, 413.
Irene, E. A., 1982c, J. Electrochem. Soc. **129**, 2594.
Irene, E. A., D. Dong, and R. J. Zeto, 1980, J. Electrochem. Soc. **127**, 396.
Irene, E. A., and R. Ghez, 1977, J. Electrochem. Soc. **124**, 1757.
Irene, E. A., and Y. J. van der Meulen, 1976, J. Electrochem. Soc. **123**, 1380.
Jorgensen, P. J., 1962, J. Chem. Phys. **37**, 874.
Jorgensen, P. J., 1967, J. Electrochem. Soc. **114**, 820.
Kassner, T. F., L. C. Walters, and R. E. Grace, 1966, *Proceedings of Symposium on Thermodynamics with Emphasis on Nuclear Materials and Atomic Transport in Solids* (IAEA, Vienna), Vol. 2, p. 357.
Khoi, N. N., W. W. Smeltzer and J. D. Embury, 1975, J. Electrochem. Soc. **122**, 1495.
Kliewer, K. L., and J. S. Koehler, 1965, Phys. Rev. **140**, 1226A.
Kofstad, P., 1966, *High Temperature Oxidation of Metals* (Wiley, New York).
Kofstad, P., 1972, *Nonstoichiometry, Diffusion and Electrical Conductivity in Binary Metal Oxides* (Wiley, New York).
Kofstad, P., and K. P. Lillerud, 1980, J. Electrochem. Soc. **127**, 2410.
Kofstad, P., and K. P. Lillerud, 1982, Oxid. Met. **17**, 177.
Kröger, F. A., 1974, *The Chemistry of Imperfect Crystals,* 2nd ed. (North-Holland, Amsterdam), Vol. 3.
Kröger, F. A., 1983, in *High-Temperature Corrosion,* edited by R. A. Rapp, NACE 6 (National Association of Corrosion Engineers, Houston), p. 89.
Lawless, K. R., 1974, Rep. Prog. Phys. **37**, 231.
Lees, D. G., and J. M. Calvert, 1976, Corros. Sci. **16**, 767.
Lesage, B., and A. M. Huntz, 1980, Scr. Metall. **14**, 1143.
Lie, L. N., R. R. Razouk, and B. E. Deal, 1982, J. Electrochem. Soc. **129**, 2828.
Lillerud, K. P., and P. Kofstad, 1980, J. Electrochem. Soc. **127**, 2397.

Lillerud, K. P., and P. Kofstad, 1982a, Oxid. Met. **17**, 127.
Lillerud, K. P., and P. Kofstad, 1982b, Oxid. Met. **17**, 195.
Liu, H.-T., A. F. Armitage, and D. P. Woodruff, 1982, Surf. Sci. **114**, 431.
Lloyd, I. K., and H. K. Bowen, 1981, J. Am. Ceram. Soc. **64**, 744.
Mills, T. G., and F. A. Kröger, 1973, J. Electrochem. Soc. **120**, 1582.
Mitchell, D. F., and M. J. Graham, 1982, Surf. Sci. **114**, 546.
Mitchell, D. F., P. B. Sewell, and M. Cohen, 1976, Surf. Sci. **61**, 355.
Mitchell, D. F., P. B. Sewell, and M. Cohen, 1977, Surf. Sci. **69**, 310.
Mitchell, D. F., R. J. Hussey, and M. J. Graham, 1983, J. Vac. Sci. Technol. A **1**, 1006.
Moseley, P. T., G. Tappin, and J. C. Rivière, 1982, Corros. Sci. **22**, 69.
Mott, N. F., 1981, Proc. R. Soc. London Ser. A **376**, 207.
Mott, N. F., 1982, Philos. Mag. A **45**, 323.
Moulson, A. J., and J. P. Roberts, 1961, Trans. Faraday Soc. **57**, 1208.
Mrowec, S., 1967, Corros. Sci. **7**, 563.
Mrowec, S., and K. Przybylski, 1977, Oxid. Met. **11**, 365.
Muehlenbachs, K., and H. A. Schaeffer, 1977, Can. Mineral. **15**, 179.
Norton, F. J., 1961, Nature **191**, 701.
Paladino, A. E., and W. D. Kingery, 1962, J. Chem. Phys. **37**, 957.
Perrow, J. M., W. W. Smeltzer, and J. D. Embury, 1968, Acta Metall. **16**, 1209.
Peterson, N. L., and W. K. Chen, 1980, J. Phys. (Paris), Colloq. **C-6**, 319.
Peterson, N. L., and W. K. Chen, 1982, J. Phys. Chem. Solids **43**, 29.
Peterson, N. L., W. K. Chen, and D. Wolf, 1980, J. Phys. Chem. Solids **41**, 709.
Pfeffer, R., and M. Ohring, 1981, J. Appl. Phys. **52**, 777.
Pritchard, A. M., J. E. Antill, K. R. J. Cottell, K. A. Peakall, and A. E. Truswell, 1975, Oxid. Met. **9**, 181.
Pritchard, A. M., N. E. W. Hartley, J. F. Singleton, and A. E. Truswell, 1980, Corros. Sci. **20**, 1.
Raynaud, G. M., W. A. T. Clark, and R. A. Rapp, 1984, Metall. Trans. **15A**, 573.
Razouk, R. R., L. N. Lie, and B. E. Deal, 1981, J. Electrochem. Soc. **128**, 2214.
Reddy, K. P. R., 1979, Ph.D. thesis, Case Western Reserve University.
Reddy, K. P. R., J. L. Smialek, and A. R. Cooper, 1982, Oxid. Met. **17**, 429.
Reddy, K. P. R., and A. R. Cooper, 1982, J. Am. Ceram. Soc. **65**, 634.
Reed, D. J., and B. J. Wuensch, 1980, J. Am. Ceram. Soc. **63**, 88.
Revesz, A. G., and H. A. Schaeffer, 1982, J. Electrochem. Soc. **129**, 357.
Rhines, F. N., and R. G. Connell, 1977, J. Electrochem. Soc. **124**, 1122.
Rhines, F. N., R. G. Connell, and M. S. Choi, 1979, J. Electrochem. Soc. **126**, 1061.
Rhines, F. N., and J. S. Wolf, 1970, Metall. Trans. **1**, 1701.
Rigo, S., F. Rochet, A. Straboni, and B. Agius, 1981, in *The Physics of MOS Insulators,* edited by G. Lucovsky, S. Pantelides, and F. L. Galeener (Pergamon, New York), p. 167.
Ritchie, I. M., G. H. Scott, and P. J. Fensham, 1970, Surf. Sci. **19**, 230.
Roberts, G. J., and J. P. Roberts, 1966, Phys. Chem. Glasses **7**, 82.
Rosenberg, A. J., 1960, J. Electrochem. Soc. **107**, 795.
Rosencher, E., A. Straboni, S. Rigo, and G. Amsel, 1979, Appl. Phys. Lett. **34**, 254.
Rowlands, P. C., and M. I. Manning, 1983, in *High Temperature Corrosion,* edited by R. A. Rapp, NACE 6 (National Association of Corrosion Engineers, Houston), p. 30.
Sangster, M. J. L., and D. K. Rowell, 1981, Philos. Mag. A **44**, 613.
Schaeffer, H. A., 1978, J. Mater. Sci. Lett. **13**, 1146.
Schaeffer, H. A., 1980, J. Non-Cryst. Solids **38**, 545.
Schottky, W., 1939, Z. Phys. **113**, 367.
Sheasby, J. S., and J. D. Brown, 1978, Oxid. Met. **5**, 405.
Sheasby, J. S., and D. B. Jory, 1978, Oxid. Met. **12**, 527.
Sleppy, W. C., 1961, J. Electrochem. Soc. **108**, 1097.
Smeltzer, W. W., and D. J. Young, 1975, Prog. Solid State Chem. **10**, 17.
Taft, E. A., 1978, J. Electrochem. Soc. **125**, 968.
Tammann, G., 1920, Z. Anorg. Allg. Chem. **111**, 78.
Tannhauser, D. S., 1974, in *Defects and Transport in Oxides,* edited by M. S. Seltzer and R. I. Jaffee (Plenum, New York), p. 333.
Taylor, M. R., J. M. Calvert, D. G. Lees, and D. B. Meadowcroft, 1980, Oxid. Met. **14**, 499.
Volpe, M. L., and J. Reddy, 1970, J. Chem. Phys. **53**, 1117.
Wagner, C., 1933, Z. Phys. Chem. B **21**, 25.
Williams, E. L., 1965, J. Am. Ceram. Soc. **48**, 190.
Wittenhauer, M. A., and L. L. Van Zandt, 1982, Philos. Mag. **46**, 659.
Wood, G. C., and F. H. Stott, 1983, in *High Temperature Corrosion,* edited by R. A. Rapp, NACE 6 (National Association of Corrosion Engineers, Houston), p. 227.
Yee, J., and F. A. Kröger, 1973, J. Am. Ceram. Soc. **56**, 189.
Young, D. J., and M. Cohen, 1977a, J. Electrochem. Soc. **124**, 769.
Young, D. J., and M. Cohen, 1977b, J. Electrochem. Soc. **124**, 775.
Young, D. J., and M. J. Dignam, 1973, J. Phys. Chem. Solids **34**, 1235.
Young, F. W., J. V. Cathcart, and A. T. Gwathmey, 1956, Acta Metall. **4**, 145.
Yurek, G. J., J. P. Hirth, and R. A. Rapp, 1974, Oxid. Met. **8**, 263.